UNIVERSITY OF CALGARY

Monte Carlo Scatter Estimate For High Energy Therapeutic Photon Beams

by

Gyöngyvér Bulz

A THESIS

SUBMITTED TO THE FACULTY OF GRADUATE STUDIES

IN PARTIAL FULFILLMENT OF THE REQUIREMENTS FOR THE

DEGREE OF MASTER OF SCIENCE

DEPARTMENT OF PHYSICS AND ASTRONOMY

CALGARY, ALBERTA

FEBRUARY, 2001

ABSTRACT

Knowledge of the photon energy spectrum emanating from a medical linear accelerator improves the accuracy of treatment planning and delivery in radiation therapy. A reconstruction method based on narrow beam attenuation is highly dependent upon the accuracy and precision of transmission measurements from 100 to 1 percent. The method described in this work overestimates the high-energy tail of the spectrum, which was thought to be due to the scattered radiation detected. The purpose of this study is to identify the sources of scattered radiation striking the detector so that a more accurate reconstruction of the energy spectrum can be obtained. An EGS4 Monte Carlo user code was written to estimate the amount of scatter, and to obtain the primary photon transmission only. The simulations showed that the energy of the scatter detected was less then 1% of the total energy scored implying no significant effect on the primary transmission.

ACKNOWLEDGEMENTS

I wish to acknowledge a particular debt of gratitude to my supervisor Dr. Stephen Sawchuk whose support and assistance made it possible to complete this project. He has constantly fired up my enthusiasm, shown me how to go about actually get things done.

I would also like to thank the members of my committee, Dr. Hans Laue, Dr. David Spencer, and Dr. Harold Lau for reading the thesis and providing useful comments.

My sincere thanks go to people who taught me, encouraged me and helped me over the last two years, directly or indirectly to make this project happen: my fellow students Parminder Basran and Collins Yeboah.

Last, but not least, I wish to thank my husband Liviu and my son Raul for encouraging me to develop myself and for their long endurance and constant support. Without them I could never had completed this thesis.

THIS THESIS IS DEDICATED TO MY PARENTS

Önélkülük nem jutottam volna ide.

TABLE OF CONTENTS

LIST OF FIGURES

Chapter 1

Theoretical Consideration

1.1 Introduction

1.1.1 Background of Investigation

Cancer is the leading cause of premature death in Canada. The National Cancer Institute of Canada reports that cancer is responsible for almost one third of all potential years of life lost [Statistics Canada 1999]. As the Canadian population continues to age and grow in size, there will be a corresponding increase in the number of new cases. The percentage of deaths in new cases is 49% overall. About 55% of all patients diagnosed with cancer will be treated with radiotherapy. The long-term survival of cancer patients treated with radiotherapy alone or with combined-modality treatments such as with surgery or chemotherapy is impressive for several types of cancer. The International Commission on Radiation Units of Measurements recommends that when delivering a radiation dose, the calculated dose should be within 5% of the actual dose delivered (ICRU 24, p45-50). The most widely used treatment machines are linear accelerators. These produce high-energy electrons which can be used

directly for treatment or produce high-energy X-rays for treatment of deep-seated tumors.

The precise knowledge of the photon energy spectra produced by medical linear accelerators plays an important role in the accuracy of the dose delivered to the patient in all the procedures involved in treatment planning (dose distribution in media, beam quality, beam calibration, and attenuation coefficients). The bremsstrahlung spectrum produced by a medical linear accelerator is considerably different from the ones used in research due to filters which adjust the photon beam for therapy requirements. Direct measurement of the X-ray spectra of a therapy machine is not feasible because of the high intensities and difficulty of determining the detector efficiency for high-energy photons. Different indirect methods have been developed which all suffer from the following disadvantages. Theoretical calculations based on quantum electrodynamics [Schiff 1951, Heitler 1954] are satisfactory for thin targets. Bremsstrahlung photons from linear accelerators are produced by thick targets. To shape the intensity of the beam they have to go through flattening filters. These factors affect the spectrum. Photoactivation techniques [Nath and Shultz 1976, Hirayama and Nakamura 1973] are useful only above the threshold energy for photonuclear reaction. Spectral reconstruction from Compton scattered photons [Levy *et al.* 1974] is technically difficult, and is also impractical in a clinical environment. One other method is the reconstruction of the photon energy spectrum from transmission measurements in narrow beam geometry. Also referred to as attenuation analysis, it is limited by the accuracy to which the

transmission curve can be measured. There are several complications in the measurement of the primary photon transmission. They are: scattered radiation, electrometer noise and leakage, and detector response that is energy dependent. It is important to detect the primary beam only in order to obtain an accurate reconstruction. To overcome these effects a direct Monte Carlo user code has been developed to estimate the proportion of scattered to primary signals.

1.1. 2 Thesis Objective

The techniques used for determination of the photon energy spectrum emanating from a medical linear accelerator can be divided in three categories: (1) the Monte Carlo (MC) method, (2) measurements, and (3) analytic calculations. MC calculations are built on the foundation of measured and calculated probability distributions, and provide benchmarks for analytic calculations and verification of results obtained in difficult measurement situations. The purpose of this thesis is to make treatment planning and delivery in radiation therapy more accurate by improving the reconstruction of the photon energy spectrum. MC techniques provide the most precise way to calculate the "real" attenuation. Specifically this means the simulation of the attenuation measurements in narrow beam geometry in order to estimate the proportion of scatter detected. The exact geometry of the treatment room, the source, the attenuator, the extra collimator, and the detector can be simulated using EGS4 and EGSnrc Monte Carlo codes. The goal is to obtain the primary photon beam

signal only. By doing so, the reconstruction of the photon energy spectrum will be improved significantly.

1.1.3 Original Contribution of the Thesis

Several problems studied in the thesis have not been reported before in literature:

(1) A Monte Carlo based user code has been developed to simulate the treatment room, source, attenuator, and extra collimator. This code scores the particles in a volume that corresponds to the external volume of an ion chamber detector with buildup cap.

(2) Attenuation measurements and photon energy spectrum reconstruction provide the energy spectrum input file for the different field sizes and attenuators used in the project.

(3) All characteristics of the particles (energy, position, direction cosines, charge, last region of interaction etc.) are stored in phase-space files. The phase-space files can be used as input files to further simulate the detector.

(4) The energy distribution of the scatter component is calculated.

(5) The origin of the scatter contribution is determined.

(6) The results are benchmarked by experimental measurements.

1.2 Fundamentals of the Physics in Radiation Therapy

1.2.1 Technical Development

In the past century, the development in electronics and computers has led to very advanced equipment to diagnose and treat patients with cancer. The precision with which radiation therapy is delivered has an impact on cancer cure rates. The factors influencing treatment delivery are:

- good diagnosis: realizable with CT (Computerized Tomography) and MRI (Magnetic Resonance Imaging) images,
- treatment-planning: three dimensional dose calculations, and
- treatment delivery techniques such as precise patient set-up and verification imaging.

The emphasis in radiation therapy is on high-energy beams, 4 to 25MV, produced by linear accelerators.

Medical linear accelerators are clinical megavoltage treatment machines, which use high-frequency electromagnetic waves to accelerate charged particles, such as electrons, to high energies through a linear tube. These electrons can be used directly for treatment or they can be directed to strike a target to produce high-energy x-rays for treatment of deep-seated tumors. X-ray beams of 1 MV or greater can be classified as megavoltage beams.

High-energy electrons from the wave-guide are focused on the target which is thick enough to stop electrons (Figure 1.1). The target is usually a high

Z material, such as tungsten or gold, promotes the electrons to interact creating bremsstrahlung radiation. The target backing made from a lower Z material stops the high-energy electrons, which escape the target. It is usually made of copper to provide fast heat dissipation. The primary collimator is made of heavy materials such as tungsten or depleted uranium. The opening is a circular cone with the apex located at the electron beam bombardment point. A flattening filter is placed in the x-ray beam to reduce the intensity of the forward peaked dose in the center of the field. Flattening filters are shaped to produce dose uniformity across the radiation field at a specific depth. A dose monitoring system is built into the path of the beam which monitors dose rate and beam symmetry. A light, projected via mirrors in the head of the accelerator, is arranged to be congruent with the radiation field and is used in the alignment of the radiation beam and the treatment field.

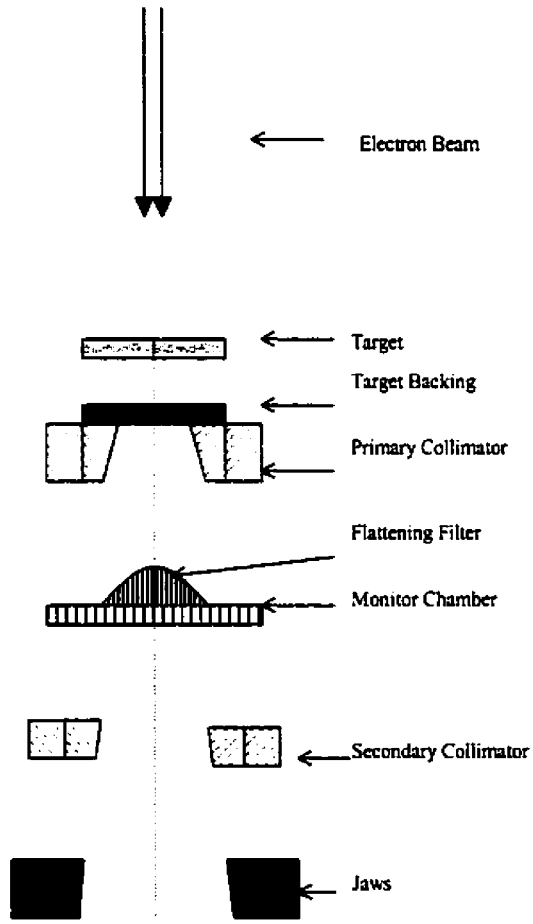

Figure 1.1 Typical head of the linear accelerator.

1.2.2 Physics of X-ray Production

There are two different mechanisms by which x-rays are produced. One gives rise to *bremsstrahlung x-rays* and the other to *characteristic x-rays* [Khan, 1994].

A. Bremsstrahlung

The process of bremsstrahlung (braking radiation) is the result of a radiative interaction between a high-speed electron and an atomic nucleus. The electron while passing near the nucleus may be deflected from its path by the action of Coulomb forces of attraction and lose energy as bremsstrahlung radiation. The electron, with its associated electromagnetic field, passes in the vicinity of the nucleus and suffers a sudden deflection and deceleration. As a result, part or all of its kinetic energy is dissociated from it and propagates in space as electromagnetic radiation.

The mechanism of bremsstrahlung production is illustrated in Figure 1.2.

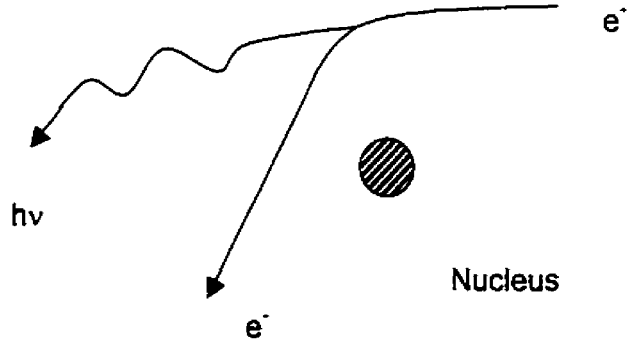

Figure 1.2 Bremsstrahlung process

Since an electron may have one or more bremsstrahlung interactions in the material and an interaction may result in partial or complete loss of electron energy, the resulting bremsstrahlung photon may have any energy up to the initial kinetic energy of the electron. The direction of emission of bremsstrahlung photons depends on the energy of the incident electron. At electron energies below about 100 keV, x-rays are emitted more or less equally in all directions [Evans, 1955]. As the kinetic energy of the electron increases, the direction of x-ray emission becomes increasingly forward.

In linear accelerators, transmission-type targets are used in which the electrons bombard the target from one side and the x-ray beam is obtained on the other side. The energy loss per atom by electrons depends on the square of the atomic number (Z^2) of the material. Thus the probability of bremsstrahlung production depends on Z^2 of the target material. The acceleration produced by a nucleus of charge, Ze, on a particle of charge, *ze*, and mass, *M*, is proportional to Zze^2/M. The accelerated charge radiates energy at the rate proportional to the square of the acceleration, in this case to $(Zze^2/M)^2$. The total bremsstrahlung per atom varies as the square of the atomic number, and varies inversely with the square of the mass of the incident particle. The efficiency of x-ray production depends on the atomic number of the target material and the megavoltage applied to the incident particle. It can be shown that the efficiency of x-ray production with tungsten target ($Z = 74$) for electrons accelerated through 100 kV is less than 1%. The rest, 99%, appears as heat, due to collisional interactions.

The average X-ray energy is approximately 1/3 of the peak voltage (kVp) of the machine.

B. Characteristic X-rays

Electrons incident on a target produce characteristic x-rays. An electron, with kinetic energy E_0, interacts with the atoms of the target by ejecting an orbital electron, such as a K, L, or M electron, leaving the atom ionized. The primary electron's kinetic energy after the collision is $E_0 - \Delta E$, where ΔE is the energy given to the orbital electron. A part of ΔE is spent in overcoming the binding energy of the electron ejected, and the rest is carried away by that electron. When a vacancy is created in an orbit, an outer orbital electron will fall to fill the vacancy. The energy difference between the two shells may be radiated in the form of electromagnetic radiation. This is called characteristic radiation because it is characteristic of the atoms in the target and the shells between which the transition took place. With higher atomic number targets, the characteristic radiation emitted may be of high enough energies to be considered as part of the x-ray spectrum. There is a threshold energy that a primary incident electron must possess to be able to eject an orbital electron and that is the binding energy. The binding energy is specific to the shell, and to the target material of the electron to be ejected.

C. X-ray Spectra

X-ray photons produced by X-ray machines are heterogeneous in energy. The energy spectrum shows continuous distribution of energies for the bremsstrahlung photons superimposed by characteristic radiation of discrete energies. The characteristic radiation is in the low kilovoltage range, therefore does not impact heavily on the spectrum for the megavoltage therapy (above 1 MV).

1.2.3 The Interactions of Photons in Matter

Photons are classified according to their mode of origin, not their energy. Thus, *γ-rays* are the electromagnetic radiation accompanying nuclear transitions, *bremsstrahlung*, or *continuous x-rays*, are the result of acceleration of free electrons or other charged particles. *Characteristic x-rays* are emitted in atomic transitions of bound electrons between the *K, L, M* shells in atoms. *Annihilation radiation* is emitted when a positron (positive electron) and an electron combine. The quantum energy of the radiation described above can be expressed as $E = h\nu$, where ν is the frequency and h is Planck's constant. Interactions of these photons with matter are thought to be independent of the mode of origin of the photon and dependent only upon its quantum energy.

The effects which photons produce in matter are almost exclusively due to secondary electrons. A photon produces primary ionization only when it removes an electron from an atom by photoelectric effect or Compton scattering.

The secondary electron can get nearly as much energy as the primary photon, producing excitations and ionization of the atoms along its path. The one primary ionization is thus completely negligible in comparison with the large amount of secondary ionization. This absorbed energy is an important quantity in radiotherapy. By absorbed energy, we mean the photon energy which is converted into kinetic energy of secondary electrons. The kinetic energy is eventually dissipated in the medium through excitation and ionization processes.

There are a number of processes which can cause photons to be scattered or absorbed. Five of the processes which will be briefly described here are: (1) photoelectric effect, (2) Compton (incoherent) scattering, (3) Rayleigh (coherent) scattering, (4) pair and triplet production, and (5) photonuclear effect. The Compton effect, the photoelectric effect, and pair production are the most important for radiation therapy, as they result in transfer of energy to electrons, which then impart that energy to matter. Rayleigh scattering is elastic scattering. In this interaction the photon changes its direction of travel by a small angle with no energy loss. Photonuclear interactions are only significant at photon energies above the ones used in radiation therapy.

(1) The Photoelectric Effect

The photoelectric effect is the phenomenon in which a photon interacts with an atom and ejects one of its orbital electrons. All of the photon energy, $h\nu$, is transferred to the electron which escapes with $h\nu - E_b$ kinetic energy, where E_b is the binding energy of the electron. Interactions of this type can take place with

electrons in the *K, L, M, ...* shells. The vacancy can be filled by an outer orbital electron with the emission of characteristic radiation or Auger electrons. The characteristic radiation is described above. Auger electrons are outer shell electrons which receive enough energy from the atom to escape. The energy obtained by the atom is derived from the difference in potential energies when an inner shell vacancy is filled by an outer shell electron.

The *K*-shell electrons, which are the most tightly bound, are the most important in the energy range of medical and biological interest. If the photon energy is below the binding energy of a given shell, an electron from that shell cannot be ejected. In particular for medium *Z* and high-*Z* elements, a plot of total mass attenuation coefficient versus photon energy exhibits the characteristic absorption edges. As the binding energy of each electron shell is attained, the probability of the photoelectric absorption involving that given shell becomes very high. Beyond that point the probability of photoelectric attenuation decreases approximately as $1/(h\nu)^3$ until the next absorption edge.

Theoretical treatment of the photoelectric effect is tedious and difficult because the Dirac relativistic equation for a bound electron must be used. Because of the restricted and approximate character of the theoretical results, the quantitative aspects of the photoelectric effect are largely empirical.

The absolute probability of a photoelectric interaction is described by the *atomic cross section* τ_a ($cm^2/atom$). Cross section data was published by Hubbell [1969], empirically determined, and later published by Scofield [1973, 1985], and

Hubbell and Seltzer [1995]. The photoelectric cross section dependence upon Z and $h\nu$ is given by

$$\tau_a \cong const.Z^n/(h\nu)^m \tag{1.1}$$

$n \cong 4$ at $h\nu = 0.1$ MeV, gradually increasing to about 4.6 at 3 MeV

$m \cong 3$ at $h\nu = 0.1$ MeV, gradually decreasing to about 1 at 5 MeV [Hubbell, 1999]

(2) The Compton Effect

The Compton effect is the phenomenon by which the photon interacts with an atomic electron as if it were "free". The "free" means that the binding energy of the electron is much less than the energy of the bombarding photon. In this interaction, the electron receives some energy from the photon and is emitted at angle ϕ with regard to the direction of incident photon. The photon with reduced energy, is scattered at angle θ. The Compton process can be analyzed in terms of an elastic collision between the two particles, the incident photon and the "free" electron. Energy and momentum conservation laws apply. The kinetic energy of the Compton electron is given as:

$$E = h\nu[\alpha(1-\cos\theta)]/[1+\alpha(1-\cos\theta)] \tag{1.2}$$

where:

$$\alpha = h\nu/m_0c^2 \tag{1.3}$$

$h\nu$=incident photon energy

and, m_0c^2≡rest energy of the electron (m_0c^2 = .511 MeV)

In 1928, Klein-Nishina successfully applied Dirac's relativistic theory of the electron to this problem and obtained a general solution

$$\frac{d\sigma}{d\Omega} = \left[\frac{d\sigma}{d\Omega}\right]_0 \cdot F_{KN} = \frac{r_0^2}{2}\left(1+\cos^2\theta\right)\cdot F_{KN} \qquad (1.4)$$

where:

$$F_{KN} = \left\{\frac{1}{1+\alpha(1-\cos\theta)}\right\}^2 \cdot \left\{1+\frac{\alpha^2(1-\cos\theta)^2}{[1+\alpha(1-\cos\theta)](1+\cos^2\theta)}\right\} \qquad (1.5)$$

For $\alpha = 0$, or $\theta = 0$ equation (1.5) reduces to the classical Thomson scattering expression. To obtain the total cross section, equation (1.5) must be multiplied by the element of solid angle $d\Omega = 2\pi \sin\theta\, d\theta$ and integrated over all angles of θ.

To consider the real situation we must take into account that electrons are in motion and energy is required to eject them from the atom. The incoherent scattering function $S(x,Z)$ takes care of that, in which x is a momentum transfer variable related to the incident photon energy and the deflection angle of the scattered photon. Compilation of $S(x,Z)$ was done by Hubbell et all [1975]. Therefore the total cross section is:

$$\sigma = \int_{\theta=0}^{\pi} \frac{r^2}{2}\left(1+\cos^2\theta\right)\cdot F_{KN}\cdot S(x,Z)\cdot 2\pi\cdot\sin\theta\cdot d\theta \qquad (1.6)$$

The total cross section given by (1.6) can be determined graphically or by numerical integration [Hubbell, 1999]. The Compton cross section is almost independent of atomic number. This is because the atomic cross section, σ_a, is the atomic number times the electronic cross section, σ_e, i.e.,

$$\sigma/\rho = \sigma_a N/A = \sigma_e (Z/A) \cdot N \tag{1.7}$$

and $Z/A \cong ½$ for all elements except hydrogen, for which is $Z/A \cong 1$.

The cross section decreases with increase in energy. This is the most dominant interaction mechanism in tissue-like materials in the range of 100keV to 10MeV photon energies.

(3) Rayleigh Scattering

Coherent scattering, also known as classical scattering or Rayleigh scattering, is the process by which photons are scattered by bound electrons and in which the atom is neither ionized nor excited. The photon loses only a negligible fraction of its energy, since the recoil is by the entire atom including the nucleus, rather than by individual atomic electrons as in the Compton effect. Since the scattering is peaked in the forward direction, particularly at high energies, this cross section is neglected sometimes from photon transport computations.

For compilations of μ / ρ in the medical and biological region of interest, the coherent scattering cross section is computed by numerical integration of the Thomson (1906) formula weighted by $F^2(x, Z)$, where $F(x, Z)$ is the atomic form factor, and x is the momentum transfer variable dependent on the incident photon energy and the deflection angle of the scattered photon.

(4) Pair and Triplet Production

Pair production is the phenomenon in which the photon interacts strongly with the electromagnetic field of the atomic nucleus and gives up all of its energy in the creation of a positron–electron pair. This is an example of the conversion of energy into mass. The threshold energy for pair production is 1.022 MeV, which is the rest energy of the newly created particles. The total energy of the electron–positron pair is given by:

$$h\nu = \left(T_{-} + m_0 c^2\right) + \left(T_{+} + m_0 c^2\right) \tag{1.8}$$

where T_- and T_+ are the kinetic energy of the negatron and positron, respectively, and $m_0c^2 = 0.511\ MeV$ is the electronic rest energy. The most probable distribution of energy is for each particle to acquire half the available kinetic energy, although any energy distribution is possible.

Triplet production is pair production in the field of an atomic electron. The resulting particles in motion are the positron–electron pair and the atomic electron involved in the interaction. Thus, the atomic electron is also ejected from

the atom. From conservation of momentum it can be shown that the minimum photon energy for triplet production has to be $4\ m_0c^2 = 2.044\ MeV$.

The cross section for pair production varies approximately as the square of the nuclear charge *Z*. The cross section for triplet production varies as *Z* times the square of the unit charge. Tabulations of these cross sections are provided for all elements $Z = 1$ to 100 over the photon energy range *1Mev* to *100 GeV* in Hubbell *et al* [1980].

(5) Photonuclear Effect

The photonuclear effect is the phenomenon by which a high-energy photon interacts with the atomic nucleus with the result of the emission of one or more nucleons. In most cases, this process results in the emission of neutrons by the nuclei. The photonuclear effect occurs at high photon energies, usually above 10MeV, and depends on the atomic number of the material (*Z*). According to Hubbell [1998], it has a peak between 5 and 40MeV and it contributes between 2% (high Z-elements) and 6% (low Z-elements) to the total cross section. The photonuclear cross section is not included in the total cross section of the interactions in radiotherapy.

1.2.4 The Interactions of Charged Particles with Matter

Charged particles undergo a large number of interactions with small energy losses. The probability of a charged particle passing through a layer of matter without any interactions is nil. A *1MeV* electron would typically interact 10^5 times before losing all its energy [Berger 1963].

A charged particle surrounded by its Coulomb electric force field interacts with one or more electrons or with the nucleus of practically every atom it passes. These charged particle Coulomb force interactions can be characterized in terms of the relative size of the classical impact parameter *b* vs. the atomic radius *a*. For $b \gg a$ they are called "soft" collisions. For $b \cong a$ they are called "hard" or "knock-on" collisions. Coulomb force interactions with the external nuclear field will occur if $b \ll a$ with the result of bremsstrahlung photons.

(1) Soft Collisions

If the distance of closest approach of the particle to the atom with which it interacts is large compared with atomic dimensions, the atom as a whole reacts to the Coulomb field of the passing particle. This results in the transfer of a very small amount of energy (a few eV) to an atom of the absorbing medium. Soft collisions are the most numerous type of charged particle interaction and they count for roughly half of the energy transfer to the absorbing medium [Attix 1986].

(2) Hard Collisions

If the distance of the closest approach is of the order of atomic dimensions, the interaction is between the charged particle and one of the atomic electrons. This process results in ionization of the atom and an energetic secondary (knock-on) electron. The secondary electrons are called δ-rays and they undergo their own Coulomb force interactions. Although hard collisions are few in number compared to soft collisions, the fractions of the primary particle's energy that are spent by these two processes are generally comparable.

(3) The Radiative Process

If the distance of the closest approach is smaller than the atomic radius then the charged particle trajectory is deflected by the Coulomb field of the nucleus. This results in the emission of a bremsstrahlung photon. The photon may be of any energy up to the kinetic energy of the charged particle.

Collision loss varies with Z and radiative loss varies with Z^2. Hence, radiative losses are more important in high Z material. As the electron energy increases, the collision loss increases logarithmically ($ln\ E$) whereas radiative losses increase with E. Therefore at high energies radiative losses dominate.

(4) "In Flight" Annihilation and Annihilation "at Rest"

The positron travelling through matter excites and ionizes atoms just the same as the electron until it is finally brought to rest.

When a slow positron approaches close to an electron, they annihilate each other, and their masses are converted into 1.022MeV of energy. This energy appears as two photons, each with energy 0.511MeV, traveling in opposite directions from the annihilation site.

The positron is unlikely to be captured by an electron until it is nearly at rest, but if this does happen its kinetic energy will be added to the radiation energy released. This is an example of mass converted to energy and it is the opposite of pair production.

1.2.5 Stopping Power for Charged Particles

The term, stopping power, refers to energy loss by electrons per unit path length in a material. According to ICRU [1980], the total mass stopping power, S/ρ , of a material for charged particles is the quotient of dE by ρdl, where dE is the energy lost by a charged particle traversing a distance dl in the material of density ρ, i.e.

$$S/\rho = dE/(\rho \cdot dl) \tag{1.9}$$

where S is the total linear stopping power. For energies at which nuclear interactions can be neglected, the total mass stopping power is

$$S/\rho = 1/\rho\{(dE/dl)_{col} + (dE/dl)_{rad}\} \tag{1.10}$$

where $(dE/dl)_{col}$ is the linear collision stopping – power and $(dE/dl)_{rad}$ is the linear radiative stopping power.

The linear collision stopping power is the rate of energy loss resulting from the sum of the soft and hard collisions. The soft collision term was derived by Bethe based on the Born approximation, and improved by Berger and Seltzer [1983]. The mass collision stopping power for electrons and positrons were obtained by combining Bethe's soft collision formula with a hard-collision relation based on Møller cross section for electrons or the Bhabba cross section for positrons as discussed by Evans [1955].

The derivation of the mass radiative stopping power is based on the theory of Bethe and Heitler as discussed in Evans [1955].

An extensive set of calculated values of mass stopping powers has been published by ICRU [1984b].

1.2.6 Basic Methods in Radiation Dosimetry

The ionization chamber is the most widely used type of dosimeter for precise measurements, such as those required in radiotherapy. The typical order of magnitude of charge or current to be measured from ionization chambers can be best estimated from the fact that an exposure of 1R generates a charge of $\equiv 3 \times 10^{-10}$C in 1cm^3 of room temperature air at a pressure of 1 atm. In most practical cases, currents lie in the range 10^{-6} to 10^{-14}A. For photon measurements the wall of the chamber must be at least as thick as the maximum range of the electrons present, to provide Charged Particle Equilibrium (CPE) and keep out stray electrons. Charged particle equilibrium exists for a volume *v* if each charged particle of a given type and energy leaving *v* is

replaced by an identical particle of the same energy entering, in terms of expectation values [Attix, 1983].

Chapter 2

Calculations and Measurements

2.1 Photon Beam Attenuation

A well-collimated, monoenergetic photon beam shows an exponential absorption in matter. This is because photons are absorbed or scattered in a single event.

2.1.1 Exponential Attenuation

Consider a *monoenergetic* parallel beam consisting of a very large number N_0 of photons incident perpendicularly on a flat plate of material of thickness x as shown in Figure 2.1.

Attenuation describes the process by which photons are removed from a narrow beam through absorption or scattering. The fractional change in N due to absorption of particles in dx is:

$$dN/N = -\mu \cdot dx \qquad (2.1)$$

where:

μ - is the linear attenuation coefficient depending upon (E, Z)

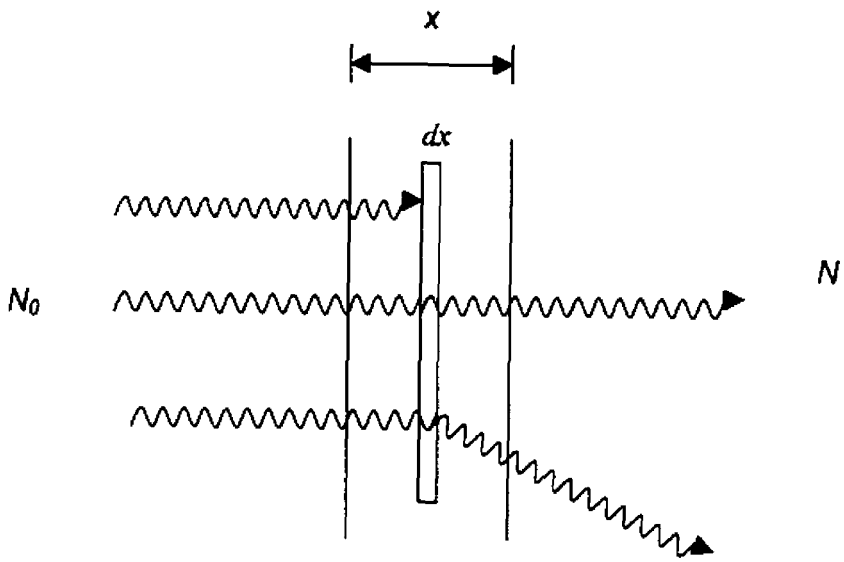

Figure 2.1 Photon attenuation

Integrating over the thickness of the absorber from *0* to *x*, and the corresponding particle population from N_0 to *N*:

$$\int_{N=N_0}^{N} \frac{dN}{N} = -\int_{x=0}^{x} \mu \cdot dx \tag{2.2}$$

$$\frac{N}{N_0} = e^{-\mu x} \tag{2.3}$$

Equation 2.3 describes the exponential attenuation.

The probability of a photon (x-ray, gamma-ray, bremsstrahlung, etc.) of a given energy *E* undergoing absorption or scattering when traversing a layer of material Z can be expressed quantitatively in terms of the ***linear attenuation coefficient*** μ (cm^{-1}). Since μ is dependent on the material's density, ρ ($g\ cm^{-3}$), the quantity usually tabulated is the mass attenuation coefficient, μ/ρ (cm^2g^{-1}), in which the dependence on the density has been removed.

Calculations of photon interaction data are generally in terms of *atomic cross sections*, in units of cm^2/atom, customarily in units of barns/atom where 1barn =$10^{-24}cm^2$. The total atomic cross section σ_{tot} is related to the total mass attenuation coefficient according to:

$$\mu/\rho\left(cm^2g^{-1}\right) = \sigma_{tot}\left(cm^2/atom\right)/(u(g)\cdot A) \tag{2.4}$$

where u(g) =1.6605402x10^{-24}g is the atomic mass unit , which is defined as 1/12 of the mass of an atom of the nuclide ^{12}C, and A is the relative atomic mass of the target element.

The total atomic cross section σ_{tot} can be written as the sum over the cross section for the most probable individual processes by which photons interact with atoms:

$$\sigma_{tot} = \tau + \sigma_{incoh} + \sigma_{coh} + k_{pair} + k_{trip} + \sigma_{ph.n.} \qquad (2.5)$$

where

τ - photoelectric effect cross section

σ_{incoh} - Compton (incoherent) scattering cross section

σ_{coh} - Rayleigh (coherent) scattering cross section

K_{pair} - pair production (in the field of nucleus) cross section

K_{trip} - triplet production (in the field of electrons) cross section, and

$\sigma_{ph.n.}$ - photonuclear cross section

Current compilations of the mass attenuation coefficient μ/ρ are derived from theoretical and empirical values of the cross section for the individual processes according to:

$$\mu/\rho = (\tau + \sigma_{incoh} + \sigma_{coh} + k_{pair} + k_{trip})/(u(g) \cdot A) \qquad (2.6)$$

The photonuclear cross section has been omitted from μ/ρ compilations up to the present, even though it has a resonance peak between 5 and 40 MeV and it can contribute between 2% (high Z elements) and 6% (low Z elements) to the total cross section. In the photon energy range of most interest in medical and biological applications, 5KeV to a few MeV, the envelope of uncertainty of μ/ρ is of the order 1% to 2% [Hubbell, 1999].

The quantity $1/\mu$ (cm or m) is known as the ***mean free path*** of the primary particles. It is the average distance a single particle travels through given attenuating medium before interacting. It is also the depth to which a fraction $1/e$ ($\cong$ 37%) of a large homogeneous population of particles in a beam can penetrate.

2.1.2 Narrow Beam Attenuation

The exponential attenuation described above will be observed for a monoenergetic beam of photons which are absorbed without producing scattered or secondary radiation. Real beams of photons interact with matter by processes that may generate charged or uncharged secondary radiation, as well as scattering primaries either with or without loss of energy.

The scattered and secondary photons can be either counted in N or not. If they are counted then equation (2.3) becomes invalid in describing the variation of N vs. x. Such cases are referred to generally as ***broad-beam attenuation***. If the scattered or secondary photons reach the detector, but only

the primaries are counted in *N*, we have ***broad-beam geometry*** but ***narrow-beam attenuation***. Equation (2.3) is valid under this condition even for real beams of photons. If the scattered radiation cannot reach the detector then equation (2.3) is valid and we talk about ***narrow-beam geometry***.

One of the methods of reconstruction of the photon energy spectrum from transmission measurements uses narrow beam geometry. The photon beam is collimated to be just large enough to cover the detector uniformly, thereby minimizing the number of secondary or scattered particles generated in the attenuator. The radiation beam source is located at a large distance from the attenuator so that the particles are almost perpendicularly incident. A secondary collimator will prevent photons scattered by a few degrees (S) from reaching the detector as shown in Figure 2.2.

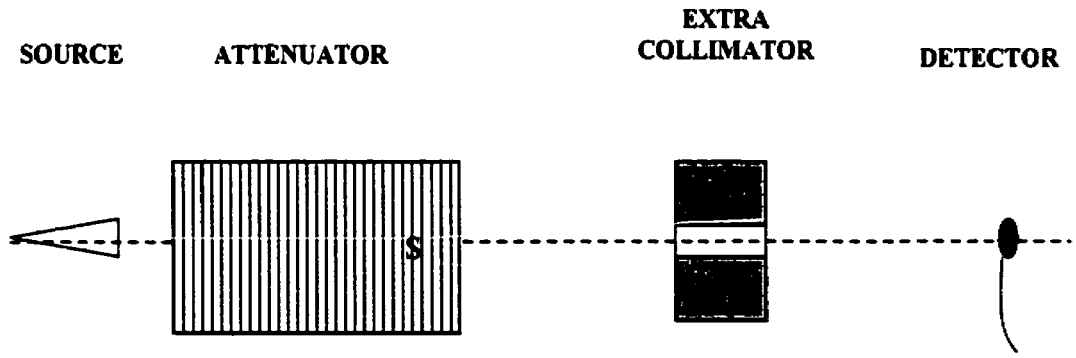

Figure 2.2 Narrow beam geometry

It is not difficult in practice to achieve reasonable narrow-beam geometry experimentally. Thus, narrow-beam attenuation can be closely approximated as

required. Transmission measurements with different attenuators with varying thicknesses, and for different photon energies are described in the literature [Huang *et al*, 1983; Catala *et al*, 1993, 1995 etc.]

2.2 X-ray Spectral Reconstruction From Transmission Data

The photon spectrum determination of a medical linear accelerator can be done from a transmission curve measured under narrow beam conditions. Narrow beam geometry is used to reduce the scatter detected. The method is based upon obtaining a carefully measured transmission curve. The best results are obtained if the transmission curve extends below 1% of the open signal. The relative transmission function, $T(x)$, is defined as the ratio of the signals

$$\frac{S(x)}{S(0)} = T(x) = \int_{E_{min}}^{E_{max}} exp[-\mu(E)\cdot x]\cdot F(E)\cdot dE \qquad (2.7)$$

where

$S(0)$ ionization measured in absence of absorber

$S(x)$ ionization measured with absorber of thickness x

$\mu(E)$ linear attenuation coefficient of the considered attenuator for the energy E

$F(E)$ fraction of the signal corresponding to the photons of energy between E and $E+dE$ in unattenuated beam

E_{min} minimum energy of the spectrum, and

E_{max} maximum energy of the spectrum

Equation (2.7) can be solved accurately by approximating it with a 4^{th} order Simpson's rule. It is discretized in terms of the energy E and attenuator thickness x and transformed into a linear system of order n. The discretization yields:

$$T(x) = \sum_{i=1}^{n} \alpha_i \, exp\left[-\mu(E_i) \cdot x\right] \cdot F(E_i) \qquad (2.8)$$

where the α_i are coefficients of Simpson's Rule and $F(E_i)$ are approximated by the

constants:

F_i where $0 \le i \le n$

and F_i fall into the interval

$E_0 \le E_i \le E_n$

For n different attenuator thicknesses we can write the matrix equation:

$$\overline{T} = \underline{A} \cdot \overline{F} \qquad (2.9)$$

More explicitly we have the inverse problem:

$$\overline{F} = \underline{A^{-1}} \cdot \overline{T} \qquad (2.10)$$

Thus, the unknown spectrum components can be obtained from the known attenuation coefficient and the measured transmission vector.

The choice of the attenuator is essential in the uniqueness of the solution. For most attenuators, the variation of the attenuation coefficient with energy first decreases monotonically from 100 keV to a few MeV passing by a minimum value and then increasing. The condition to obtain a unique physical solution of the system is that the energy corresponding to the minimum value of μ must be greater than the maximum energy of the spectrum and that the linear attenuation coefficient be monotonic in the photon energy range of the x-ray spectrum.

2.3 Measurements

2.3.1 Materials and Equipment used

The measurement set-up is done in narrow beam geometry. The source, attenuator, extra collimator and detector are aligned along the central ray of the beam. The detector was placed at a sufficiently large distance from the attenuator in order to not detect larger angle scatter. The set-up for aluminum attenuator is shown in Figure 2.3

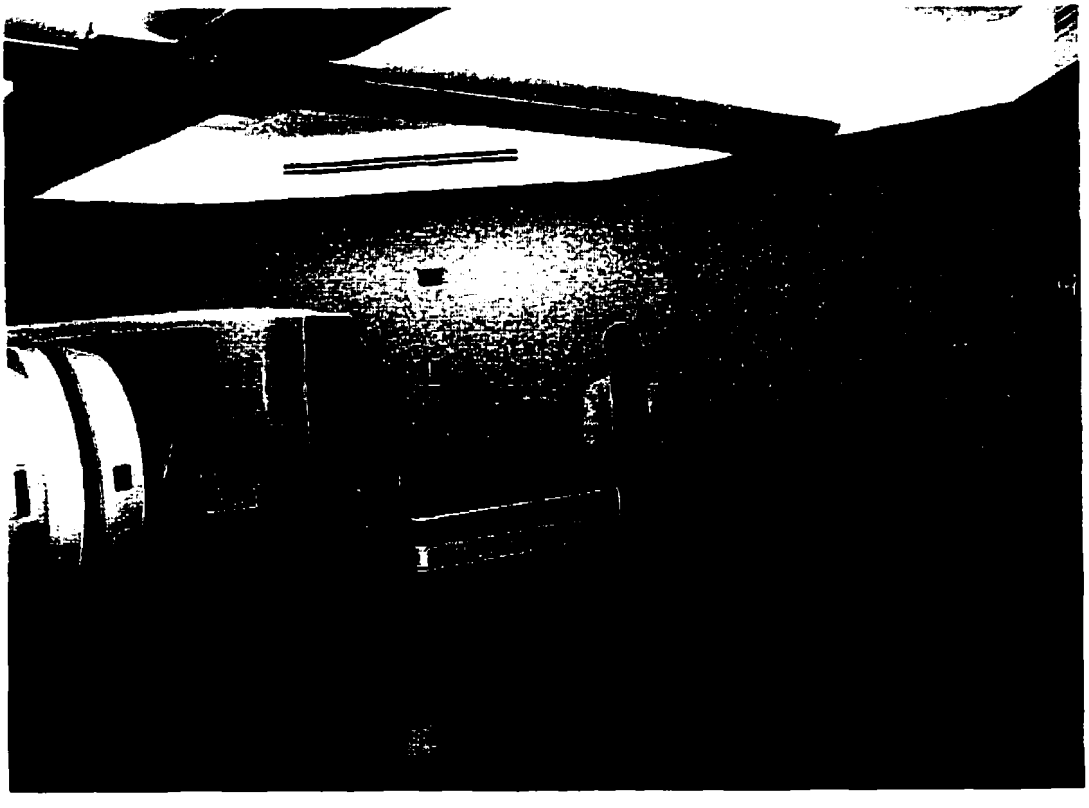

Figure 2.3 Set-up for measurements

Two types of attenuators were used: aluminum (Al) and water (H_2O) for the 6MV photon energy spectrum. These were chosen because they both satisfy the property that the linear attenuation coefficient is monotonic in the photon energy range of the x-ray spectrum. Figures 2.4 and 2.5 represents the total mass attenuation coefficients for water and aluminum [Evans, 1955]. The attenuation coefficient for H_2O is monotonically decreasing up to about 30MeV, and the one for Al to about 10MeV.

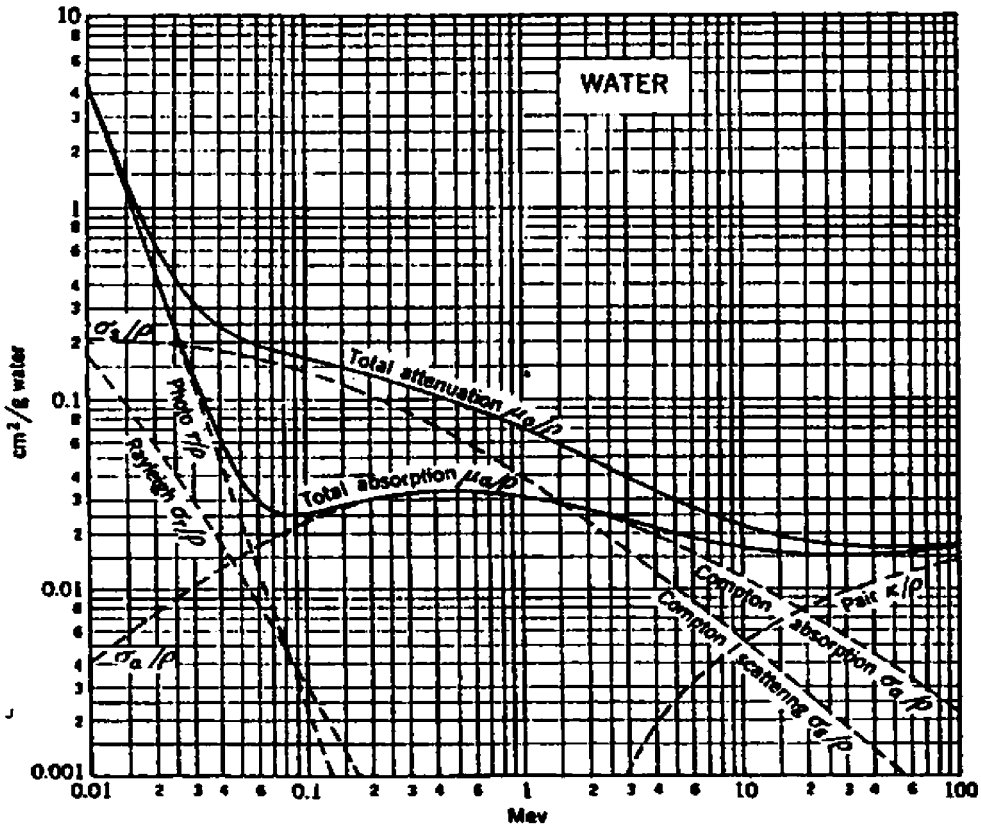

Figure 2.4 Mass attenuation coefficients for photons in water

(without permission R. D. Evans – The Atomic Nucleus – 1955)

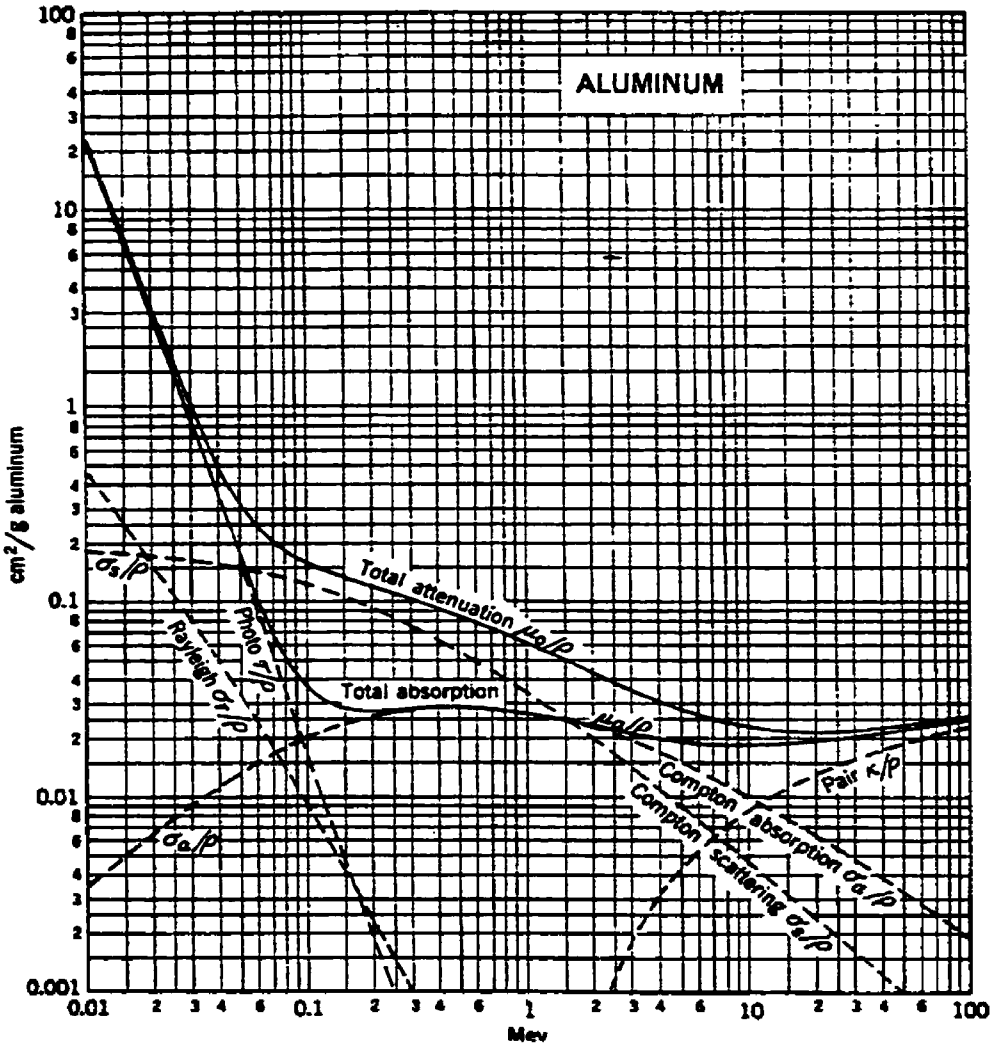

Figure 2.5 Mass attenuation coefficients for photons in aluminum

(without permission R. D. Evans – The Atomic Nucleus – 1955)

Components:

- **Aluminum attenuator:** consist in 15x15cm^2 aluminum plates with 6.37mm average thickness. Each plate's thickness was measured and recorded and the plates labeled. The attenuator thickness can be calculated with an accuracy of 10^{-2}mm. The density of the plates was 2.7 g/cm^3.
- **Water attenuator:** 14cm diameter plastic tube which was filled with water to create the desired attenuator thickness.
- **Extra collimator:** 10x10x10cm^3 cerrobend block with a 3cm diameter hole through the center.
- **Ionization chamber:** Capintec PR-05P Model 192 with 0.07ml collection volume. The attainable display resolution of the Capintec chamber is 0.01R and R/min. The walls and central pin are made of Air Equivalent Plastic (AEP). The connection cable is a Capintec Low Noise Triaxial Cable, 2.5 m long typical, with BNC Size Male Triaxial Connector. Stem effect: less than ±1%. Leakage: less than 10^{-14}A. Polarization time: 5 minute typical. Beam soaking time: one minute typical.
- **Buildup cap:** 3.5mm thick brass cylinder with one end closed used for maximizing signal.
- **Electrometer:** Keithley Model: 35040.
- **Source:** Varian CLINAC linear accelerator.

Characteristics of the materials of the various components:

impurities 0.12% Mn, 5% Mg and 0.12% Cr or alloy 61601 with impurities 0.5% Si and 0.6% Mg.

For a 6 MV photon beam the dominant interaction is Compton scattering which is almost independent of the atomic number, as described in Chapter 1. Even for lower energies where the photoelectric effect is the dominant interaction the simulation was not affected by the presence of the impurities. The photoelectric cross section depend on the atomic number, but the principal impurity for the 5056 alloy is Mg which has the atomic number Z=12 very close to Z=13 for the aluminum. Therefore, the simulation was not affected by the small total percentage impurities.

The cerrobend used for the extra collimator has the following composition: Bismuth (Bi) 50%, lead (Pb) 26.7%, tin (Sn) 13.3%, and cadmium (Cd) 10%.

2.3.2 Field Sizes, Distances and Alignment

Two different field sizes were used: 1x1cm^2 and 2x2 cm^2 measured at 100cm Source to Axis Distance (SAD). The attenuator was set up at 75cm Source to Surface Distance (SSD), the extra collimator at 230cm SSD and the detector at an approximate 330cm SSD.

The gantry of the linear accelerator was rotated to 90^0 (or 270^0) in order to obtain a horizontal beam. The attenuator and extra collimator were set up on the couch. The couch can be rotated to the position required to make the alignment of various components used possible. All components were leveled and centered using the field lights, cross hairs, and lasers.

The extra collimator was centered checking the circularity of the central hole with a piece of film or thin paper using the field lights. The ionization chamber was positioned with its central point on the x-ray beam axis with the collecting electrode oriented perpendicular to the beam. Polystyrene blocks were used to hold the various components. A piece of film was placed behind the detector and the polystyrene support. The film showed no influence of the polystyrene block on the intensity of the field.

2.3.3 Measurements

The field size was set to 1x1cm^2 at 100 SSD and the energy of the machine was set to 6MV x-rays. The chamber was irradiated using 300 monitor units (MU) at a rate of 600 MU/min. First we measured the transmission signal for the open beam (without attenuator), and then for various attenuator thicknesses. Finally the open beam was measured again to check for the consistency of the first set. During the transmission data acquisition, two readings were done for each attenuator thickness, and five readings for the open beam. About 15 transmission points were measured for each curve. A small variation of the reading without the attenuator was observed. The final readings were about 1.7% lower than the initial readings. This variation can be related to temperature variation of the different accelerator components.

In some of the previous photon spectra reconstruction publications [e.g. P.H. Huang *et al*, 1983] a protection around the chamber was used in order to eliminate the radiation scatter from the back wall and other room structures. We

did not use any protection because that can introduce more back scatter than the wall.

The measurement was repeated for the $2x2cm^2$ field and for both field sizes using the water attenuator.

The transmission curves from the measurements are presented in Chapter 4.

Chapter 3

Monte Carlo Simulation of Radiation transport

3.1 Introduction

The EGS4 code system [Nelson *et al* , 1985] originally was developed at the Stanford Linear Accelerator Centre (SLAC) for high energy physics applications; version 4 was then specifically adapted to treat low energy problems. The Monte Carlo method implemented in Electron Gamma Shower 4 (EGS4) is widely accepted as the most accurate method for doing calculations involving electrons and photons. EGS4 was designed to simulate the flow of electrons and photons through matter in a user-defined geometry at energies ranging from just below 1 MeV to several thousands of GeV. EGS4 uses a statistical game-playing approach to solve the difficult mathematical problem posed by particle transport through matter. The program uses MC simulations to predict the statistical outcomes of each interaction. All possible outcomes of an interaction are identified and assigned to an imaginary roulette wheel to reflect predicted outcomes of the interactions. The program then accumulates the data through the entire transport process, and by simulating a large number of particle histories, information can be obtained about average values of macroscopic quantities of interest such as energy deposition. As individual histories are followed, one can obtain information about the statistical fluctuations of particular

kinds of events also and information that cannot be obtained by experimental investigations.

The EGS4 Monte Carlo based computer program has four major components:

(1) The cross-section data used for all the processes being considered in the simulation.

(2) The algorithms for the radiation transport and particle interaction.

(3) The methods for specifying the geometry and scoring the physical quantities of interest.

(4) The analysis of the data obtained during the simulation.

While components (1) and (2) mainly define the underlying physics of the simulation, components (3) and (4) can vary with individual codes and applications.

3.2 Description of the Radiation Transport – Shower Process

Electrons, as they traverse matter, lose energy by collision or radiative processes. As we described earlier the result of the collision process is an excited or ionized atom. When an orbital electron is given a significant amount of kinetic energy, that electron can create its own excitation and ionization, and it is called a δ-ray. Energy loss by bremsstrahlung radiation is fairly uniformly distributed among secondary photons of all energies from zero up to the energy of the primary particle itself. At high energies a large fraction of the electron energy is spent in the production of high-energy photons that, in turn, may

interact in the medium. One of three photo-processes dominates, depending on the energy of the photon and the nature of the medium. At high energies, pair production dominates over Compton scattering. In these two processes energy is transferred to the electrons which can create bremsstrahlung photons. This process is known as the ***electromagnetic cascade shower.***

The simulation of an electromagnetic cascade shower can be decomposed into the simulation of the transport and the interactions of a single particle. A last-in-first-out stack is used to store properties of particles which have yet to be simulated. Initially, only the incident particle is on the stack. This means that the properties of the incident particle are stored in the first position of the corresponding arrays. The basic strategy is to transport the top particle until an interaction takes place, or until its energy drops below a predetermined cutoff energy, or until it enters a particular region of space. In the latter two cases, the particle is taken off the stack and the simulation continues with the next particle on top. If an interaction occurs and if there is more than one product particle, the particle with the lowest energy is put on the top of the stack and then transported. When a particle is removed from the stack and none remain, the simulation of the shower event (history) is complete.

Photons travel in a straight line with constant energy between interactions. They are transported simulating all interactions. Ranges for charged particles are often computed using the Continuous Slowing Down Approximation (CSDA) where electrons are assumed to lose energy continuously along their track, with

a mean energy loss per unit path length given by the stopping power. Multiple scattering and energy fluctuations are ignored in this case.

The type of interaction that is simulated is based upon the fact that the probability of occurrence of a type of interaction is proportional to the interaction cross section. After the type of interaction is selected, the parameters of the product particles are determined and stored in the stack. The portion of the code for transporting particles of the type corresponding to the top particle is entered. Multiple elastic scattering of charged particles is treated according to Molière's theory [Bethe, 1953]. Continuous energy loss between discrete interactions is calculated along the paths of particles. The cross sections for bremsstrahlung production are taken from Koch and Motz [1959]. Cutoff energies are used to distinguish between continuous and discrete interactions. The electron and photon cutoff energies used by EGS (and set up in PEGS) are given by AE and AP, respectively. Any electron interaction that produces a delta-ray with total energy of at least AE, or a photon with energy at least AP, is considered to be a discrete event. All other interactions are considered continuous and give rise to continuous energy losses and directional changes for the electron between discrete interactions.

Due to the statistical nature of the MC method, the accuracy of the results depend on the number of histories. Thus, to cut uncertainties in half, it is necessary to run four times as many histories.

3.3 Program flow for Running EGS4

Figure 3.1 schematically shows the structure of the EGS code system for user applications. An EGS user code operates by means of:

COMMON blocks -to change values of COMMON variables

Macro definition -to redefine the predefined features

EGS or user written SUBROUTINES:

HATCH -to establish media cross section data

SHOWER -to initiate cascade

HOWFAR -to specify the simulation geometry

AUSGAB -to score and output the results

Cross sections for the user-defined media are precalculated by an independent processor program (PEGS4). The transport of electrons or photons can be simulated in any element, compound or mixture. PEGS4 creates data to be used by EGS using cross-section tables for elements 1 through 100, considering the user-defined creation cutoff energies.

The problem-specific geometry is treated in a geometry subroutine named HOWFAR. For a given particle's position and direction of motion the subroutine mainly calculates the path length to the first geometric boundary to be encountered.

The subroutine AUSGAB scores the output variables according to the user requirements. This subroutine can be called under a variety of user defined conditions.

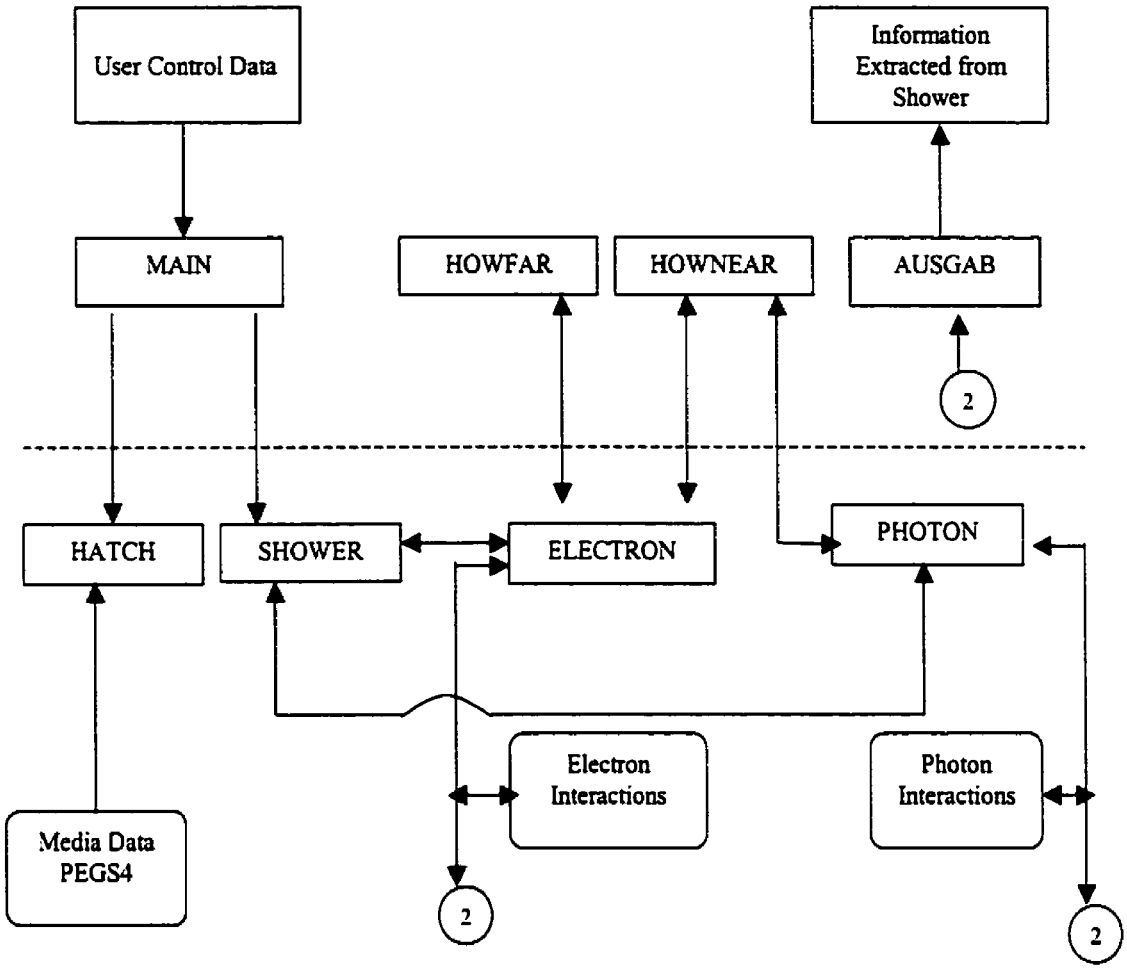

Figure 3.1 The structure of the EGS code system

3.4 The User Code Used in this Project

For medical physics and radiation dosimetry applications, various user codes have been developed to accommodate particular requirements. Several user codes developed by D.W.O. Rogers and A.F. Bielajew at the National Research Council of Canada (NRCC) have been well tested and improved by others. They are widely used in Monte Carlo calculations in radiation transport.

In this project, to simulate the photon and electron transport and to estimate the proportion of scattered to primary signal detected, the XYZDOS user code was modified and used.

XYZDOS is user a code developed to do dose deposition studies. Beams of electrons and/or photons are incident on a x-y surface at a user-defined angle. The geometry is a rectilinear volume with the origin at the bottom left, the x-y plan on the page, x directed up, y to the right, and z-axis into the page. Voxel dimensions are completely variable in all three dimensions and can be filled with different materials. The NRCC code, XYZDOS, was used as a frame to build SCATTEN.

XYZDOS is an EGS4 user code. EGSnrc is a new version of EGS4 which was released in June 2000, after SCATTEN had been finalized and checked for accuracy. In the new code system the electron transport was improved by the use of a new electron transport algorithm. Because we are interested in photon transport, the EGS4 version gives a sufficiently accurate simulation. The electrons created through the photon interactions in the attenuator are mainly locally absorbed. The energy of the charged particles scored is less the 0.02%

of the total energy scored. In this situation the new transport algorithm would not make a significant difference.

3.5 Description of the Simulation

The simulation of the narrow beam geometry was done using SCATTEN. The treatment room, the source, attenuator and extra collimator were simulated in rectilinear geometry. Transmission data for total, primary, and scatter signals were collected in a phase-space file. The scoring region was a "box" with dimensions corresponding to the outside dimensions of the buildup cap on the detector.

The phase-space files can be used as input files for future simulation of the energy deposition in the ion chamber.

Different user codes were created for the simulation of Al and H_2O attenuators for 6MV photon energy and two different field sizes.

3.5.1 Modifications of XYZDOS to SCATTEN

Materials Data File:

The materials data file used in the main program was generated using the preprocessor PEGS4. The creation cut-off energies, AE and AP, were set to 0.521and 0.01 MeV respectively. As we mentioned before, AE is the low energy threshold for knock-on electron (δ-ray) production, and AP is the low energy

threshold for bremsstrahlung production. The upper limits of energies UE and UP were set to 20MeV.

Inputs:

Separate input files were created for the following situations:

Attenuator type	Field size (cm^2)	Attenuator thickness	Detector distance (cm)
Aluminum	1x1	No attenuator 15 attenuator thickness	245cm, 330cm, 453cm
	2x2	No attenuator 15 attenuator thickness	330cm
Water	1x1	No attenuator 15 attenuator thickness	245cm, 330cm
	2x2	No attenuator 15 attenuator thickness	330cm

Main Program:

- An initial starting spectrum was used to simulate the beam spectrum and it is one that is reconstructed from attenuation measurements which are not corrected for scatter.
- The source configuration was modified to create a divergent beam.
- The subprogram HOWFAR was used to recreate the treatment room and the set-up geometry, including the floor, walls, ceiling, attenuator, extra collimator, and the scoring region in Figure 3.2. When the particle left the geometry or entered the scoring region, it is discarded by the user requesting the flag IDISC set to 1.

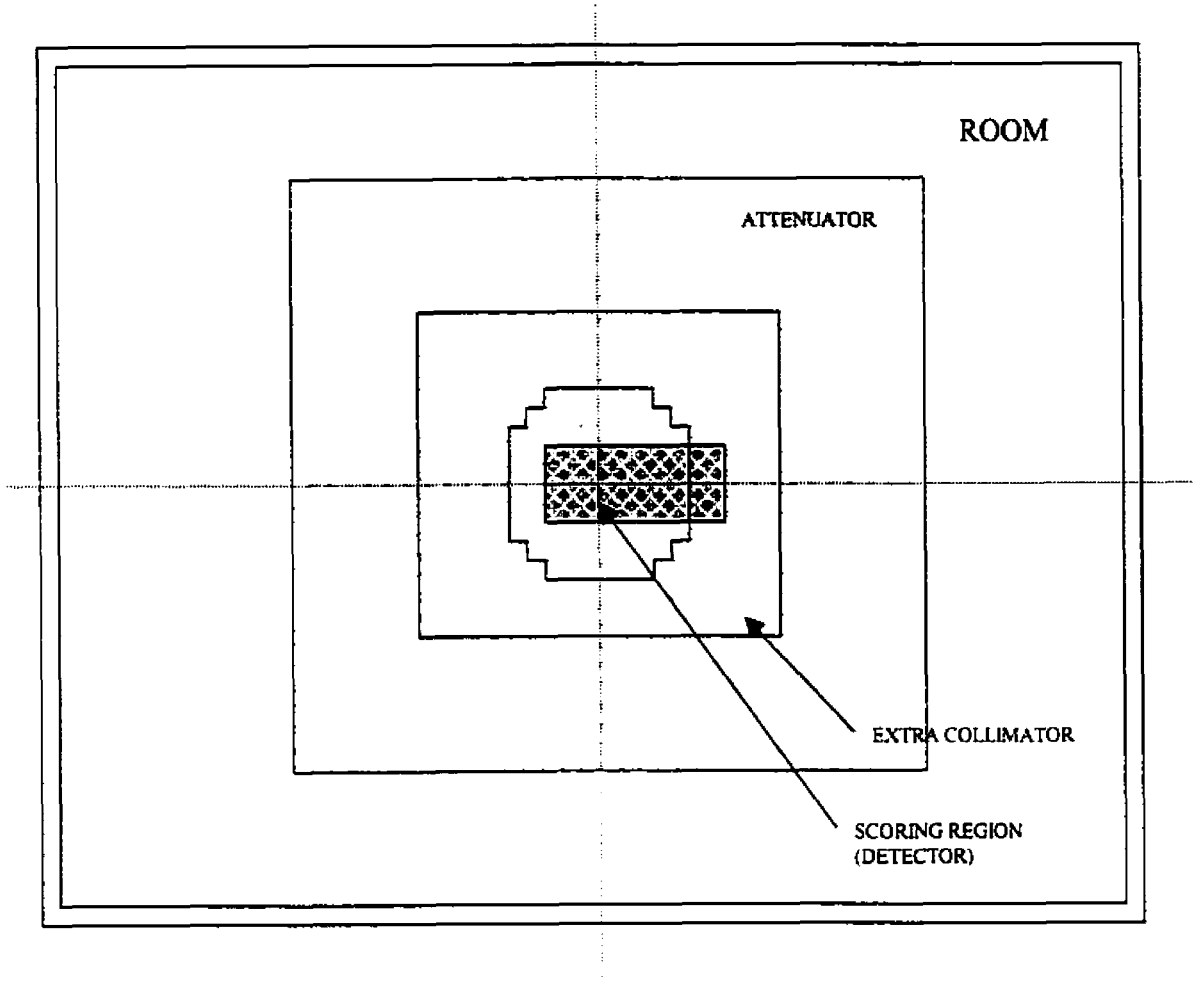

Figure 3.2 The simulated geometry (beam's eye view)

The scoring subprogram AUSGAB was modified to score the attenuation information, and to output all the information regarding the particles which reached the scoring region. To obtain this, the particles were tagged using a parameter LATCH which is contained in COMMON/STACK. LATCH can be set for any particle on the stack of the particles being transported, and it is passed on to all its progeny in this shower process. This provides a simple procedure for keeping track of the history of a particle. For example if LATCH is set for a particular incident photon which undergoes Compton scattering generating a recoil electron, which then initiates a bremsstrahlung photon, this final photon (and all other descendents of the initial particle) will have the same value of LATCH.

Flags are set to track the following events in AUSGAB:

(1) **Compton scattering** with two resulting particles: electron and photon

- Check which particle is on the top of the stack and just below.
- If the photon is on the top of the stack, then set LATCH(NP)= 2 and update the particle's region number LASTIR(NP)= IR(NP).
- If the electron is on the top of the stack, then go to the next particle on the stack, which must be the photon and set LATCH(NP-1)=2, LASTIR(NP-1)= IR(NP-1).

The electron can create a bremsstrahlung photon which we tagged in the following way:

(2) **Bremsstrahlung** with two resulting particles: electron and photon

- Check which particle is on the top of the stack and just below.

- Repeat the same tagging process as for Compton event only using a different LATCH number. See Appendix 1.

(3) **The photoelectric effect** is not tagged because in this process the photon is absorbed. The photoelectron can be scored as a charged particle if it reaches the scoring region. If the photoelectron creates a bremsstrahlung photon, this will be tagged as above.

(4) **Pair production**. If the incident photon undergoes a pair production event, the electron created will be tracked by the previous methods described. The positron eventually will annihilate therefore we have to count for the photons created in this process.

(5) **Annihilation.** Annihilation can be annihilation in flight or annihilation at rest. The latter one is a special case when the positron falls below the cutoff energy before annihilating. In this case it is assumed that it comes to rest before annihilating.

A positron can also annihilate and give off only one photon via the process. The ratio of one photon to two photon annihilation cross section is small until higher energies are reached, at which point the absolute value of the cross section is small [Messel and Crawford]. Thus, the single photon annihilation process is ignored [SLAC-265, 2000]. Both photons created in the annihilation process will be tagged with the same LATCH number: LATCH(NP)= LATCH(NP-1)= 3.

These four processes (Compton, bremsstrahlung, annihilation at rest and in flight) are all the photon interactions we are interested in.

- When the particle enters the scoring region, it will be discarded at user request by setting the flag IARG=3 in AUSGAB, and IDISC(NP)=1 in HOWFAR. The particle's energy, coordinates, direction cosines, last region, and last interaction type are output in phase-space files.

Outputs:

For each simulation we have two output files. One is the phase–space file which contains the scored particles parameters and can be used as input files for further simulations. The second type of file, the "log" file, contains the general information about each simulation. The total number and the total energy of the primary photons and the scattered radiation are scored and statistical uncertainties are calculated. These files will output the geometrical regions defined, materials and densities used, therefore they are a very useful check of the accuracy of the inputs.

3.5.2 Error Analysis

Each simulation contained 1,000,000 histories split into 10 statistical batches. The average of each scoring quantity is calculated according to

$$x_{batch\_j} = \frac{1}{N_{hist}} \cdot \sum_{i=1}^{N_{hist}} \{x_i\}_j \qquad (3.1)$$

The average over statistical batches is given by

$$\bar{x} = \frac{1}{n} \cdot \sum_{j=1}^{n} x_{batch\_j} \tag{3.2}$$

where: n=10 was the number of batches used

The variance over statistical batches is given by

$$\sigma_x^2 = \frac{1}{n-1} \cdot \sum_{j=1}^{n} \left(x_{batch\_j} - \bar{x} \right)^2 \tag{3.3}$$

Finally the error in the mean

$$\sigma_{\bar{x}} = \sqrt{\frac{\sigma_x^2}{n}} \tag{3.4}$$

is used.

3.5.3 Materials Used in the Simulation

The materials used in the simulation were air, aluminum, cerrobend, water, and concrete for the walls, ceiling and floor. Their composition was taken from the ICRU material data files and compared to the composition of the materials used in the measurements.

The cerrobend simulated has the exact composition of the material used in the extra collimator. The aluminum simulated was pure aluminum. The fact that the impurities from the aluminum plates do not change the results of the simulation was discussed earlier.

Chapter 4

Results and Conclusions

4.1 Simulation Results

The purpose of the first simulations was to compare the amount of the scattered radiation detected using two field sizes: $1x1cm^2$ and $2x2cm^2$. The detector was simulated at 330cm from the source. Unexpectedly, the scatter contribution is very low, under 1%, no matter which field size was simulated. It turned out to be better to use the small sized field for both attenuators, as shown in figures 4.1 and 4.2, because of the lower scatter contribution as expected.

The second set of simulations was performed to determine the optimum distance to place the detector in order to reduce the scatter detection. The detector was simulated at three different distances for the $1x1cm^2$ field. They were: 245cm, 330cm, and 453cm SSD. The results indicate that the best position was at 330cm SSD. This was about half of the distance between the secondary collimator and the back wall. When the detector was placed at 245cm, a higher amount of scatter from the attenuator was detected. When the detector was at 453cm, it was too close to the back wall and the back-scatter contribution increased (see Figures 4.3 and 4.4).

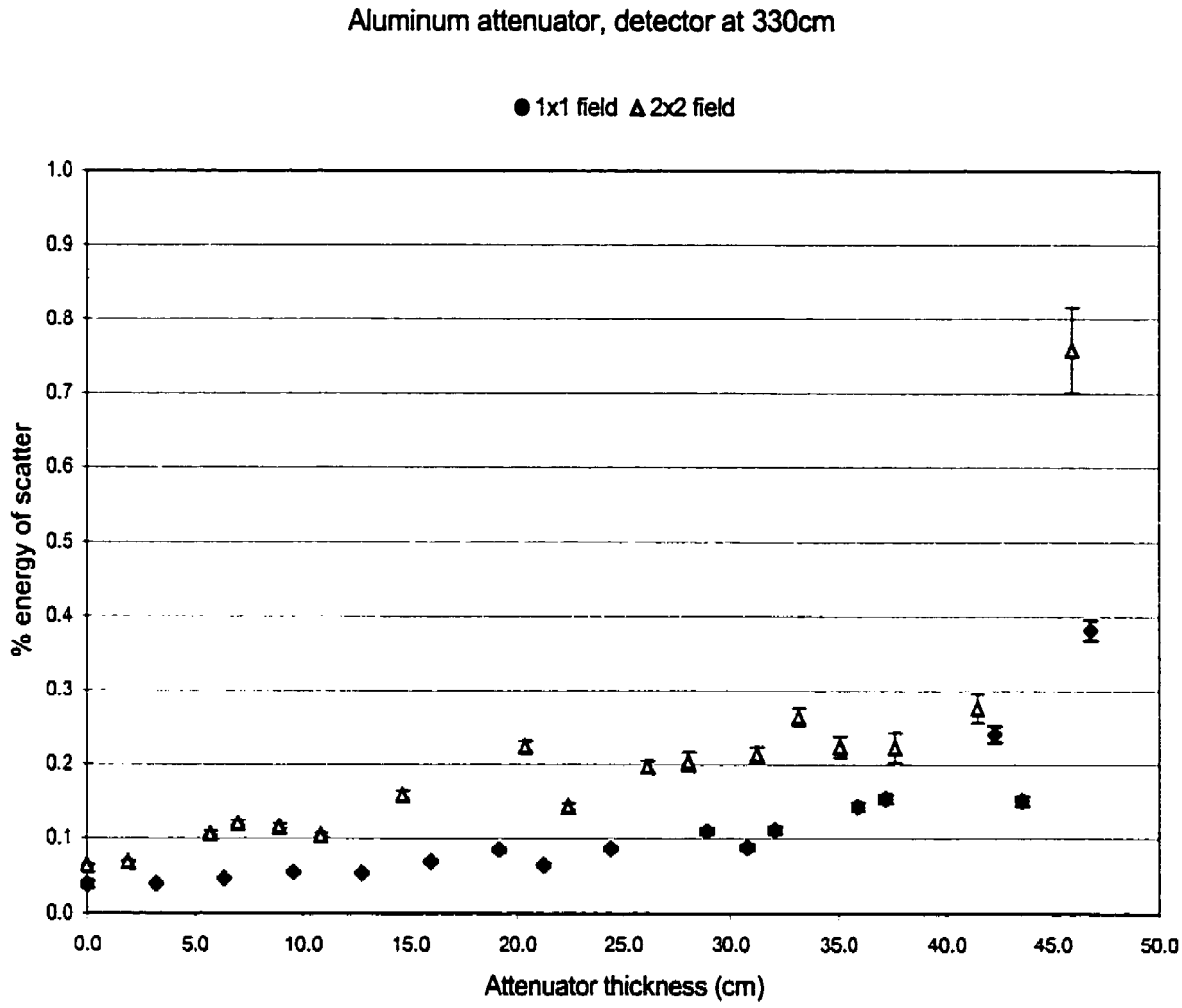
Aluminum attenuator, detector at 330cm
● 1x1 field Δ 2x2 field
% energy of scatter
1.0
0.9
0.8
0.7
0.6
0.5
0.4
0.3
0.2
0.1
0.0
0.0
5.0
10.0
15.0
20.0
25.0
30.0
35.0
40.0
45.0
50.0
Attenuator thickness (cm)

Figure 4.1

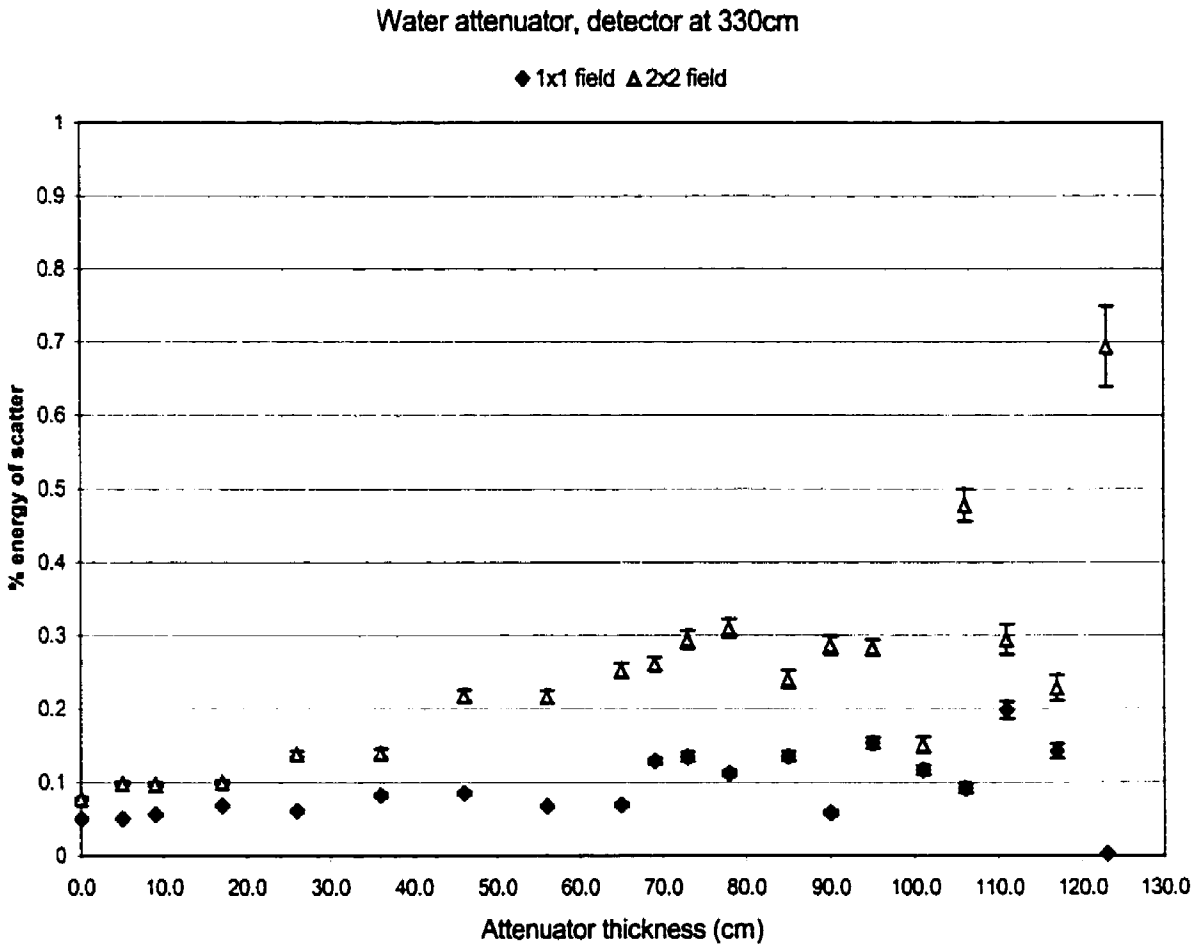
Water attenuator, detector at 330cm
◆ 1x1 field △ 2x2 field
% energy of scatter
1
0.9
0.8
0.7
0.6
0.5
0.4
0.3
0.2
0.1
0
0.0
10.0
20.0
30.0
40.0
50.0
60.0
70.0
80.0
90.0
100.0
110.0
120.0
130.0
Attenuator thickness (cm)

Figure 4.2

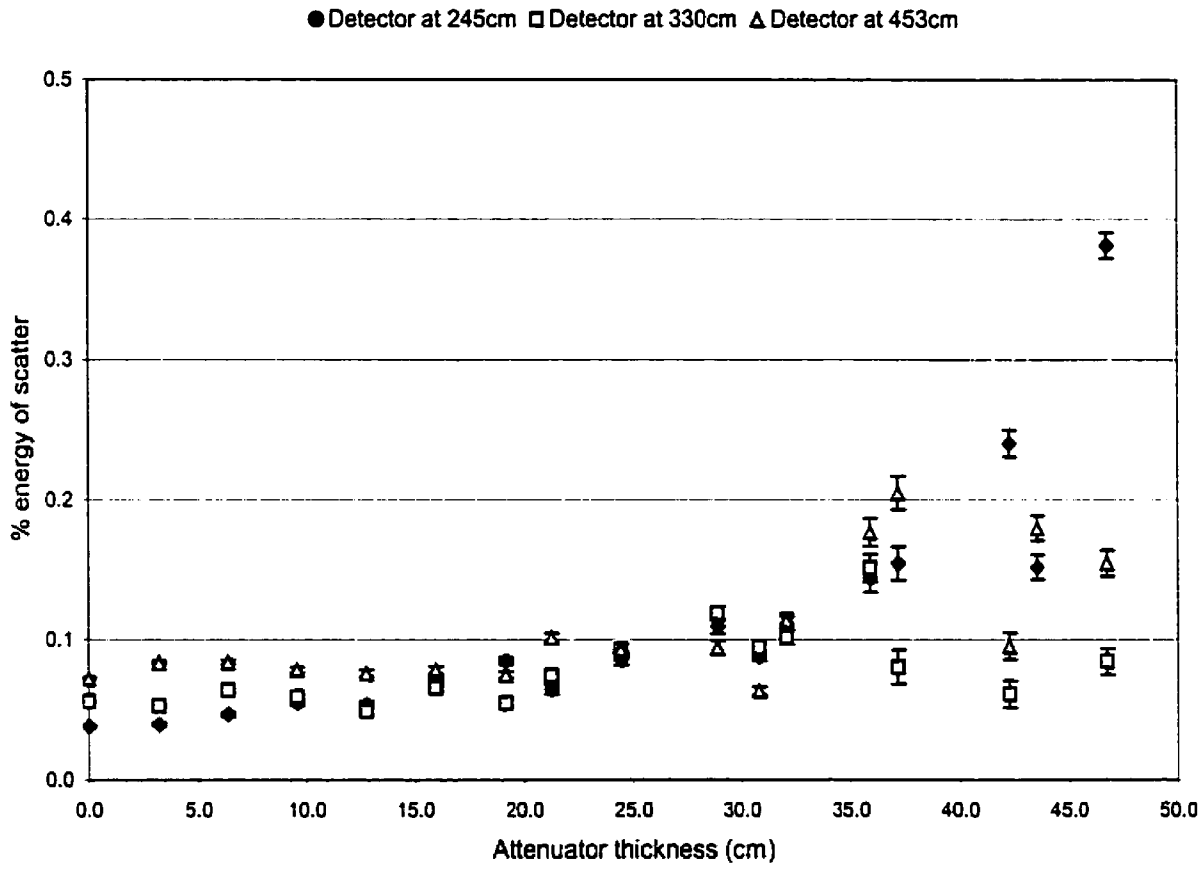
1x1 field, aluminum attenuator
Detector at 245cm
Detector at 330cm
Detector at 453cm
% energy of scatter
0.5
0.4
0.3
0.2
0.1
0.0
0.0
5.0
10.0
15.0
20.0
25.0
30.0
35.0
40.0
45.0
50.0
Attenuator thickness (cm)

Figure 4.3

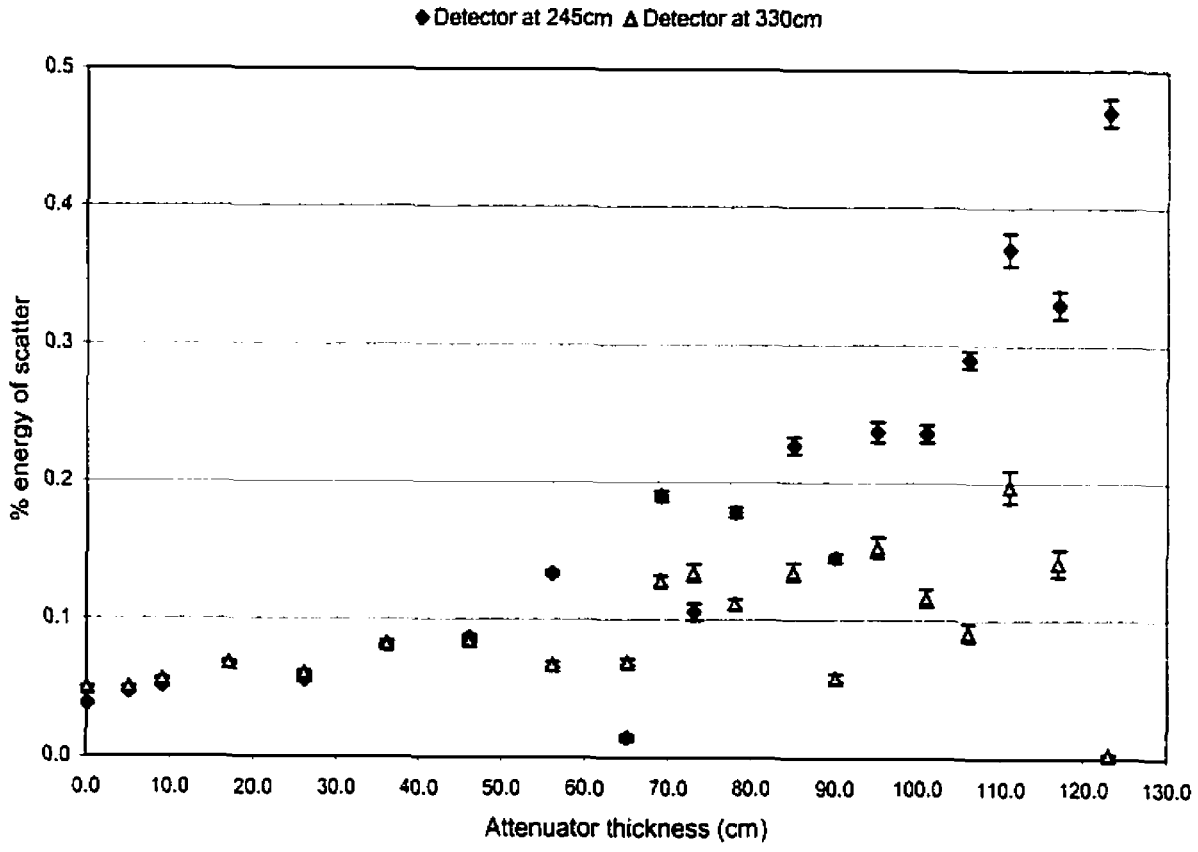
1x1 field, water attenuator
◆ Detector at 245cm △ Detector at 330cm
% energy of scatter
0.5
0.4
0.3
0.2
0.1
0.0
0.0
10.0
20.0
30.0
40.0
50.0
60.0
70.0
80.0
90.0
100.0
110.0
120.0
130.0
Attenuator thickness (cm)

Figure 4.4

These results are summarized in Table 4.1.

Table 4.1:

Field size	Attenuator	Detector distance	Scatter energy (%)	
(cm^2)		(cm)	No attenuator	Max. attenuator
1x1	Aluminum	245	0.0383 ± 2E-04	0.3813 ± 5E-04
		330	0.0561 ± 4E-04	0.0842 ± 5E-04
		453	0.0723 ± 6E-04	0.1544 ± 1E-04
2x2	Aluminum	330	0.0640 ± 9E-04	0.7587 ± 4E-04
1x1	Water	245	0.0392 ± 2E-04	0.4726 ± 8E-04
		330	0.0504 ± 2E-04	0.1417 ± 5E-04
2x2	Water	330	0.0782 ± 6E-04	0.6938 ± 4E-04

$$Scatter\_energy(\%) = \frac{Energy\_scatter\_scored}{Total\_energy\_scored} * 100$$

$$Total\_energy\_scored = Energy\_primaries + Energy\_scatter$$

The relative transmission was calculated in each simulation. The variation of the transmission calculated with and without including the energy of the scatter is presented in Table 4.2 and 4.3. The relative transmission is independent of scatter within experimental uncertainties. This is an unexpected result taking into consideration the small amount of scatter detected. Figures 4.5 and 4.6 demonstrates these results for the simulations with the 1x1cm^2 field size and the detector placed at 330cm.

Table 4.2:

Aluminum attenuator, detector at 330 cm							
1x1cm^2 field				2x2cm^2 field			
Attenuator Thickness (cm)	Transmission		Difference Between the two (%)	Attenuator Thickness (cm)	Transmission		Difference Between the two (%)
	With Scatter	Without Scatter			With scatter	Without Scatter	
0.00	1.000000	1.000000	0.0000	0.00	1.000000	1.000000	0.0000
3.20	0.735893	0.735893	-0.0032	1.91	0.832141	0.832098	0.0051
6.37	0.541655	0.541655	0.0078	5.74	0.568320	0.568079	0.0425
9.56	0.401066	0.401066	0.0030	7.01	0.509226	0.508937	0.0568
12.75	0.303479	0.303479	-0.0069	8.92	0.425641	0.425420	0.0521
15.94	0.224896	0.224896	0.0096	10.83	0.359362	0.359217	0.0403
19.13	0.170800	0.170800	-0.0013	14.65	0.253550	0.253309	0.0953
21.24	0.141099	0.141099	0.0183	20.38	0.153972	0.153725	0.1606
24.42	0.106465	0.106465	0.0369	22.39	0.128654	0.128552	0.0796
28.88	0.073775	0.073775	0.0625	26.12	0.093568	0.093443	0.1336
30.79	0.061979	0.061979	0.0382	28.04	0.077773	0.077448	0.4205
32.06	0.055841	0.055841	0.0455	31.23	0.060072	0.059982	0.1491
35.89	0.041010	0.041010	0.0950	33.14	0.052277	0.052173	0.2003
37.17	0.036057	0.036057	0.0244	35.06	0.042051	0.041984	0.1599
42.27	0.024471	0.024471	0.0051	37.61	0.034076	0.034022	0.1589
46.73	0.016743	0.016743	0.0282	41.42	0.025218	0.025165	0.2121
				45.89	0.017129	0.017010	0.7000

Table 4.3:

Water attenuator, detector at 330 cm							
1x1cm^2 field				2x2cm^2 field			
Attenuator Thickness (cm)	Transmission		Difference Between the two (%)	Attenuator Thickness (cm)	Transmission		Difference Between the two (%)
	With Scatter	Without Scatter			With scatter	Without Scatter	
0.00	1.000000	1.000000	0.0000	0.00	1.000000	1.000000	0.0000
5.00	0.814928	0.814927	0.0002	5.00	0.814319	0.814153	0.0204
9.00	0.696622	0.696580	0.0060	9.00	0.689013	0.688883	0.0189
17.00	0.512819	0.512727	0.0180	17.00	0.507477	0.507367	0.0216
26.00	0.366603	0.366564	0.0106	26.00	0.359464	0.359248	0.0601
36.00	0.252820	0.252739	0.0319	36.00	0.256454	0.256297	0.0612
46.00	0.178828	0.178766	0.0347	46.00	0.177647	0.177399	0.1395
56.00	0.126744	0.126723	0.0169	56.00	0.127708	0.127532	0.1381
65.00	0.093541	0.093523	0.0189	65.00	0.091791	0.091632	0.1742
69.00	0.081595	0.081532	0.0780	69.00	0.077612	0.077470	0.1833
73.00	0.071510	0.071450	0.0840	73.00	0.069927	0.069776	0.2164
78.00	0.060471	0.060434	0.0613	78.00	0.059154	0.059018	0.2319
85.00	0.048479	0.048438	0.0847	85.00	0.047395	0.047318	0.1619
90.00	0.040552	0.040549	0.0078	90.00	0.041757	0.041670	0.2091
95.00	0.035677	0.035640	0.1026	95.00	0.034967	0.034896	0.2054
101.00	0.028856	0.028837	0.0658	101.00	0.029960	0.029938	0.0725
106.00	0.024847	0.024836	0.0411	106.00	0.024017	0.023921	0.4016
111.00	0.021302	0.021270	0.1474	111.00	0.021095	0.021049	0.2168
117.00	0.017724	0.017707	0.0915	117.00	0.017767	0.017740	0.1503
123.00	0.014713	0.014720	-0.0475	123.00	0.014166	0.014079	0.6200

The relative transmission is independent of the distance where the detector was simulated (see Figures 4.7 and 4.8).

In this work the detector region or scoring region is a 1.347x2.9x1.347= 5.26cm^3 volume which coincides with the Capintec ionization chamber with brass buildup cap used in the measurements.

The ion collection volume of the chamber is 0.07cm^3. Analyzing the relative transmission for a small volume corresponding to the collection volume of the chamber, we find the same transmission as above (Figure4.9).

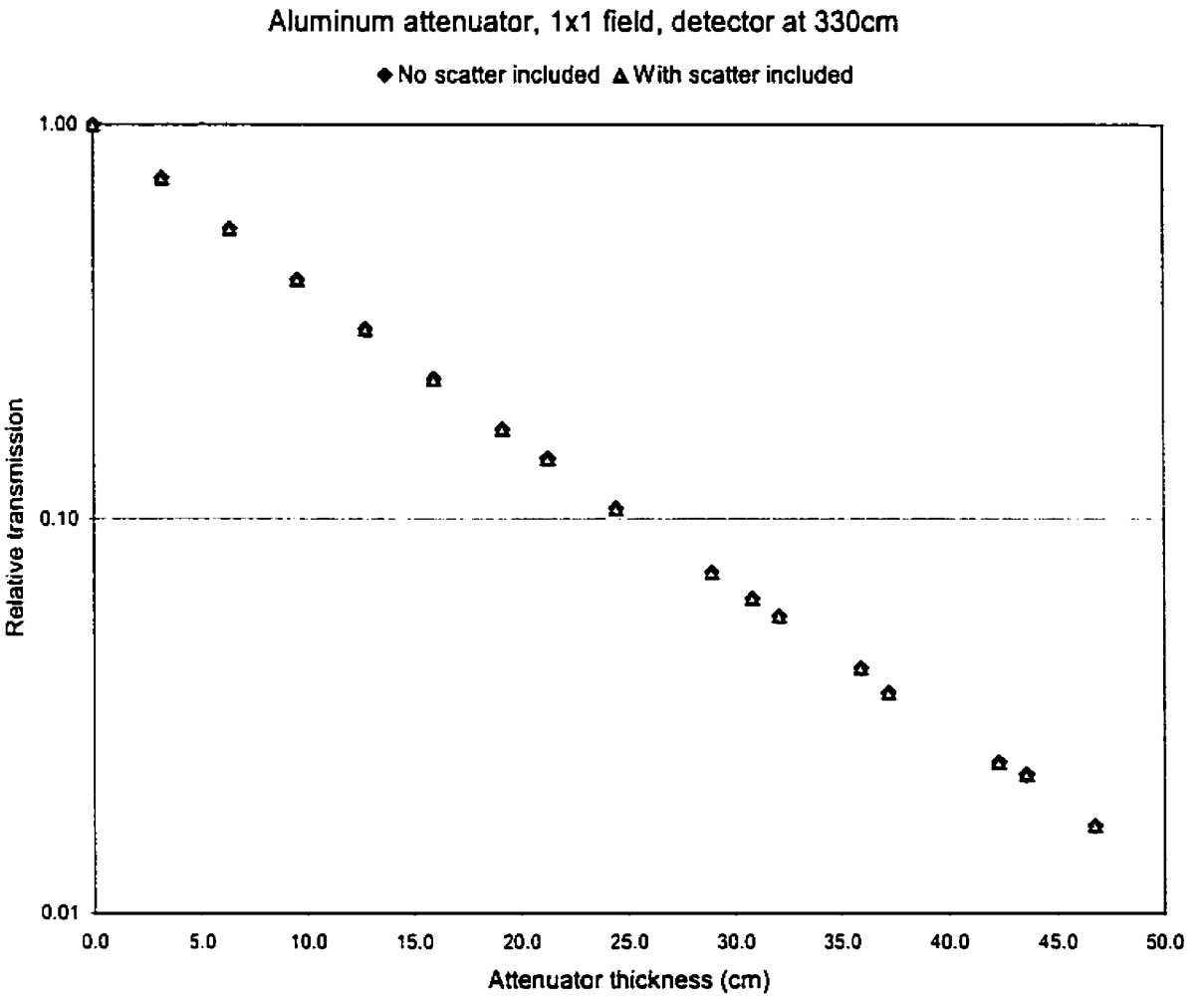
Aluminum attenuator, 1x1 field, detector at 330cm
◆ No scatter included ▲ With scatter included
1.00
0.10
0.01
Relative transmission
0.0
5.0
10.0
15.0
20.0
25.0
30.0
35.0
40.0
45.0
50.0
Attenuator thickness (cm)

Figure 4.5

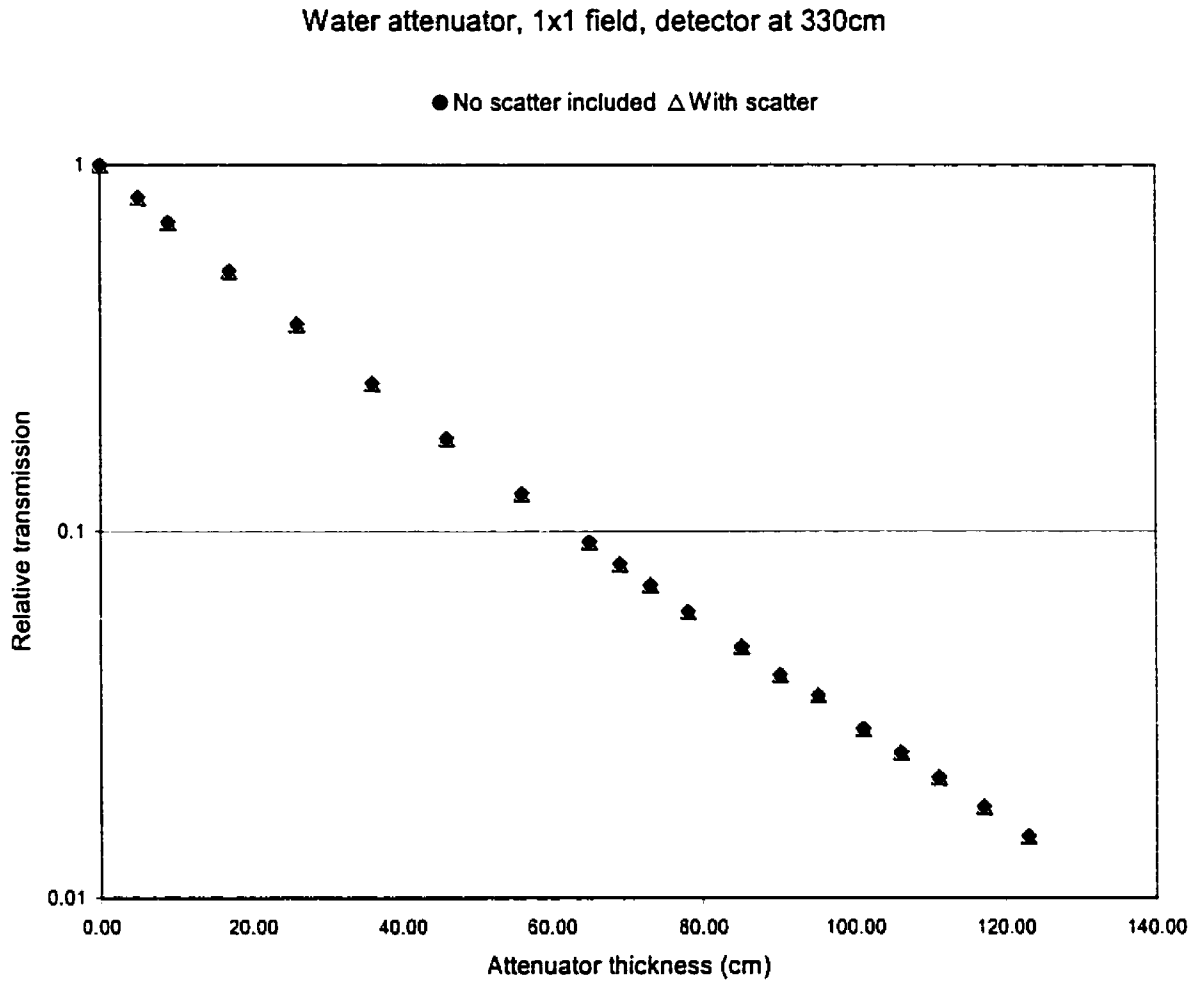
Water attenuator, 1x1 field, detector at 330cm
● No scatter included △ With scatter
Relative transmission
1
0.1
0.01
0.00
20.00
40.00
60.00
80.00
100.00
120.00
140.00
Attenuator thickness (cm)

Figure 4.6

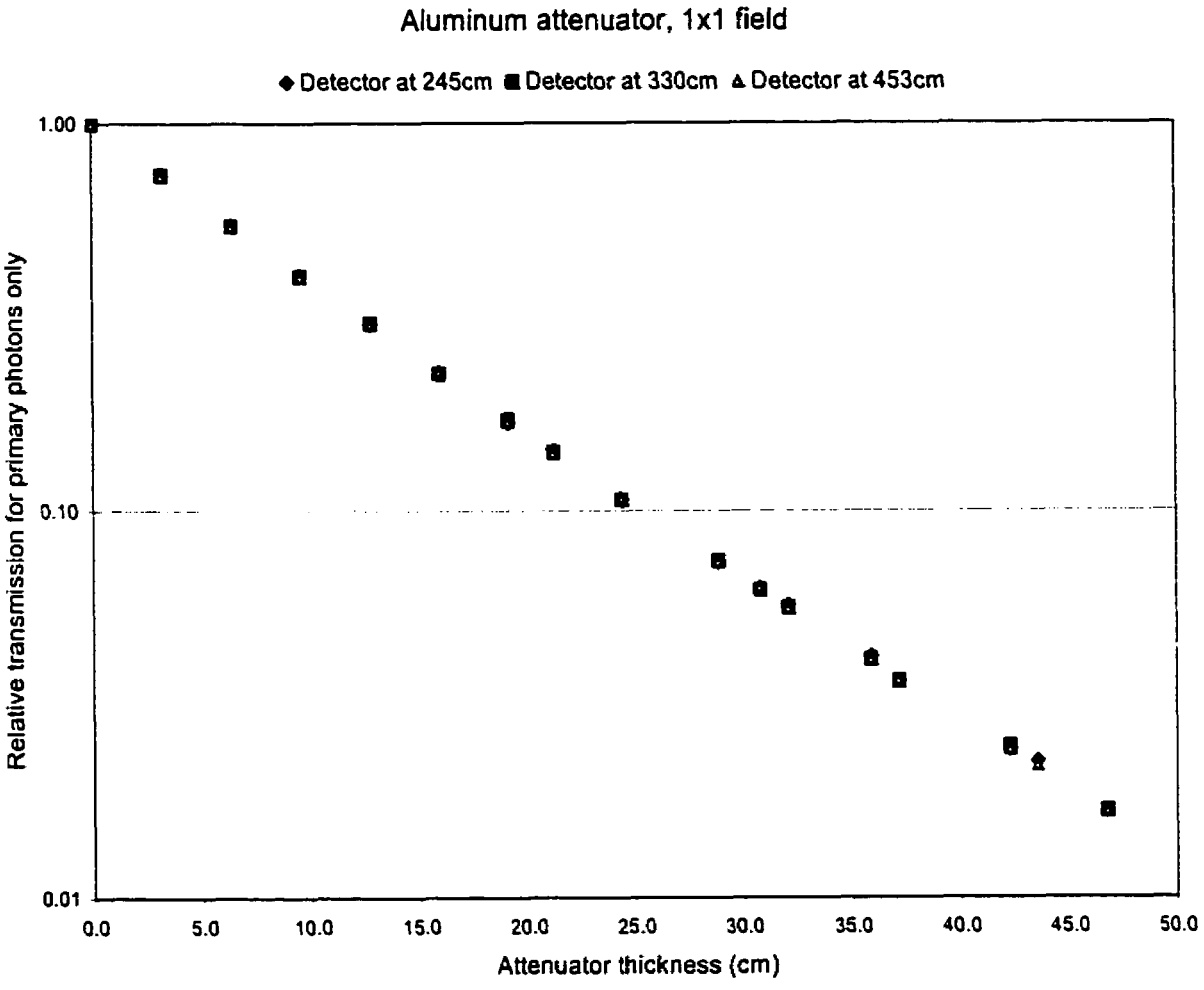
Aluminum attenuator, 1x1 field
◆ Detector at 245cm ■ Detector at 330cm ▲ Detector at 453cm
1.00
0.10
0.01
Relative transmission for primary photons only
0.0
5.0
10.0
15.0
20.0
25.0
30.0
35.0
40.0
45.0
50.0
Attenuator thickness (cm)

Figure 4.7

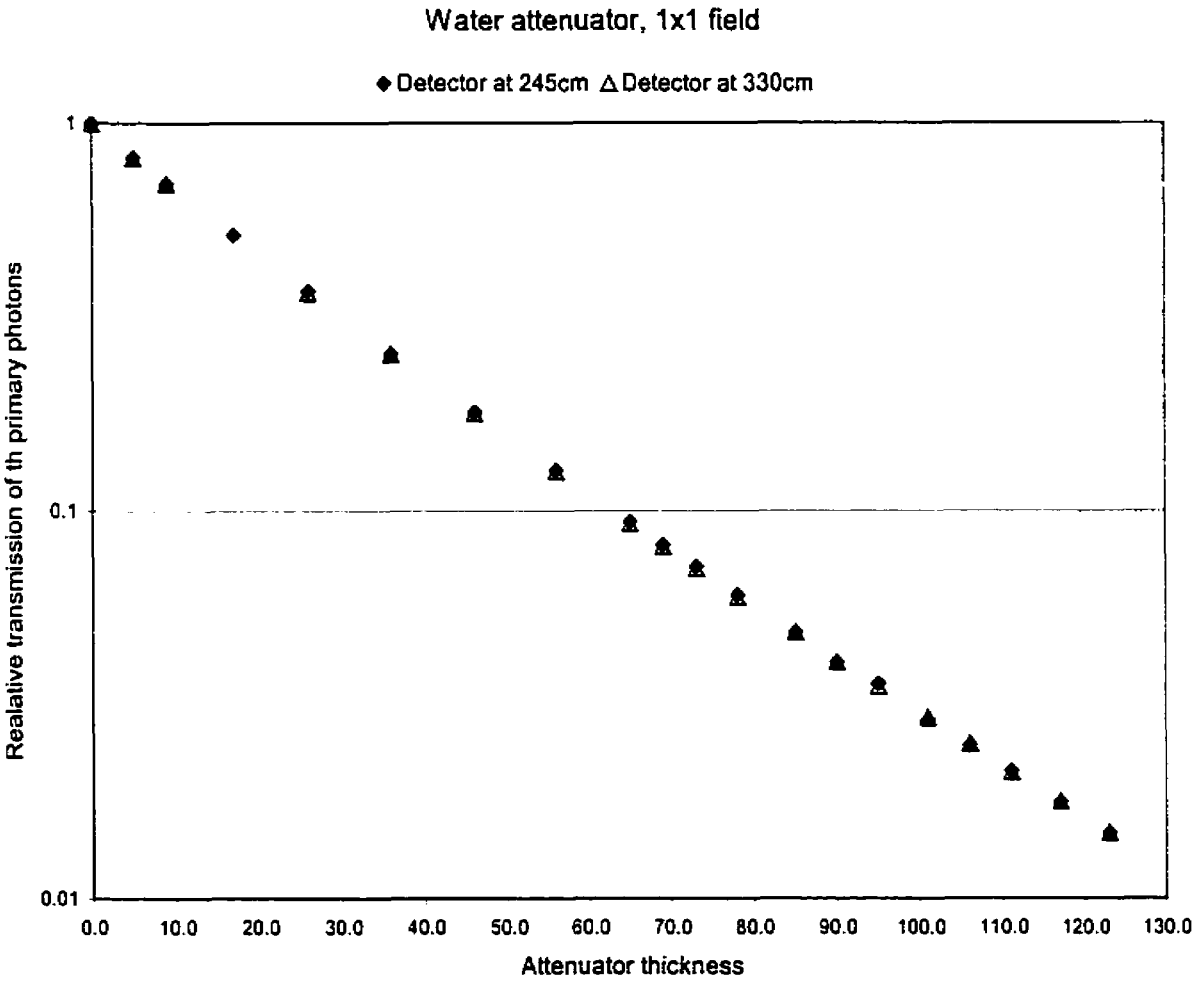
Water attenuator, 1x1 field
◆ Detector at 245cm △ Detector at 330cm
Realative transmission of th primary photons
1
0.1
0.01
0.0
10.0
20.0
30.0
40.0
50.0
60.0
70.0
80.0
90.0
100.0
110.0
120.0
130.0
Attenuator thickness

Figure 4.8

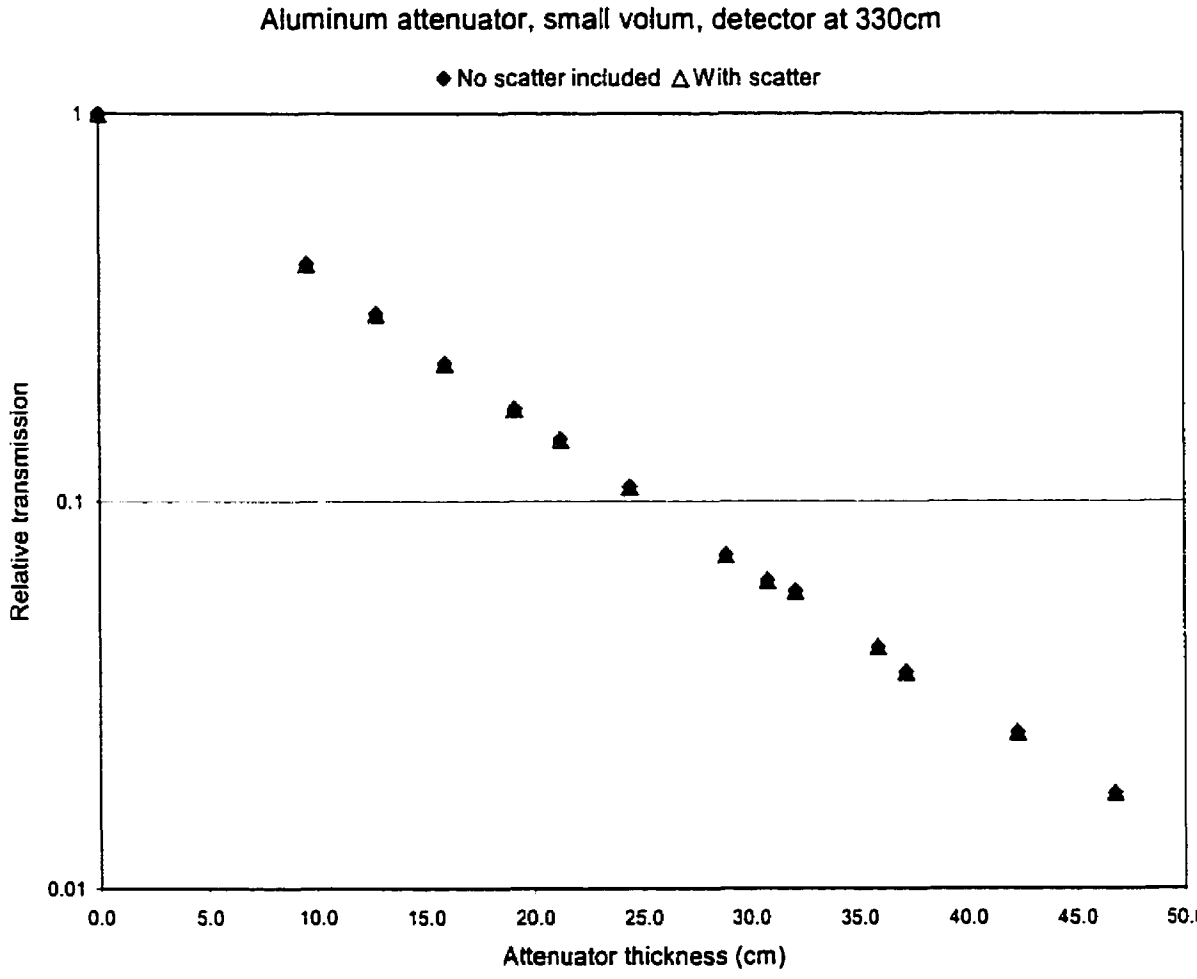
Aluminum attenuator, small volum, detector at 330cm
◆ No scatter included △With scatter
Relative transmission
1
0.1
0.01
0.0
5.0
10.0
15.0
20.0
25.0
30.0
35.0
40.0
45.0
50.0
Attenuator thickness (cm)

Figure 4.9

4.2 Comparing the Simulations with the Measurements

The measured and simulated transmission curve for aluminum and water attenuators is shown in Figures 5.2 and 5.3. The simulated transmission in both cases is higher than the measured transmission. This can be explained by looking at the original input spectrum and at the initial hypothesis. The input spectrum was reconstructed from measurements and had an overestimated high-energy tail. In a 6MV photon beam there should not be photons with energies much higher then 6MeV.

The hypothesis is that the tail of the spectrum is overestimated because of the scatter contribution. It was thought that at low transmission levels, or high photon energies, the energy of scatter detected had the same magnitude as the primary photon signal. This does not appear to be the case. As discussed earlier, the scatter contribution was always less than 1% of the total signal, which did not have a significant effect on the transmission.

New simulations were proposed in order to find the reason for the higher simulated transmission. Three modified spectra were used:

1. Spect_1: the original spectrum was modified so there were no energies above 6.25MeV. (The maximum energy of the real spectrum is 6 ± 0.18MeV.) The width of the energy bins was kept the same. The results of the simulation are lower transmission than in the original spectrum case, but still higher than the measured transmission.

2. Spect_2: the tail of the original spectrum was reshaped, dropping the probabilities for high-energy photons, and cutting energies above 7.5MeV. Finer energy bins were used. Using finer (smaller width) bins, the simulation should be more accurate because the real spectrum is continuous. The resulting transmission is lower than the one with the original spectrum used, but higher than with spect_1. My conclusion was that we have to cut the energies above 6.25 MeV.
3. Spect_3: the small, equal sized bins were kept from the previous situation. The tail of the spectrum was reshaped so no energies above 6.25MeV were kept. The resulted transmission was very close to the measured one.

For the 6MV spectrum the average energy is approximately 2MeV or 1/3 of the peak voltage of the machine. The simulations were repeated for a monoenergetic photon beam with 2MeV average energy. The result was a much lower transmission then the one obtained using the spectrum.

The energy spectra used are shown in Figure 5.1. The transmission curves obtained for aluminum and water attenuators are shown in Figures 5.2 and 5.3 respectively.

The error bars for the transmission graphs are too small to be able to see them.

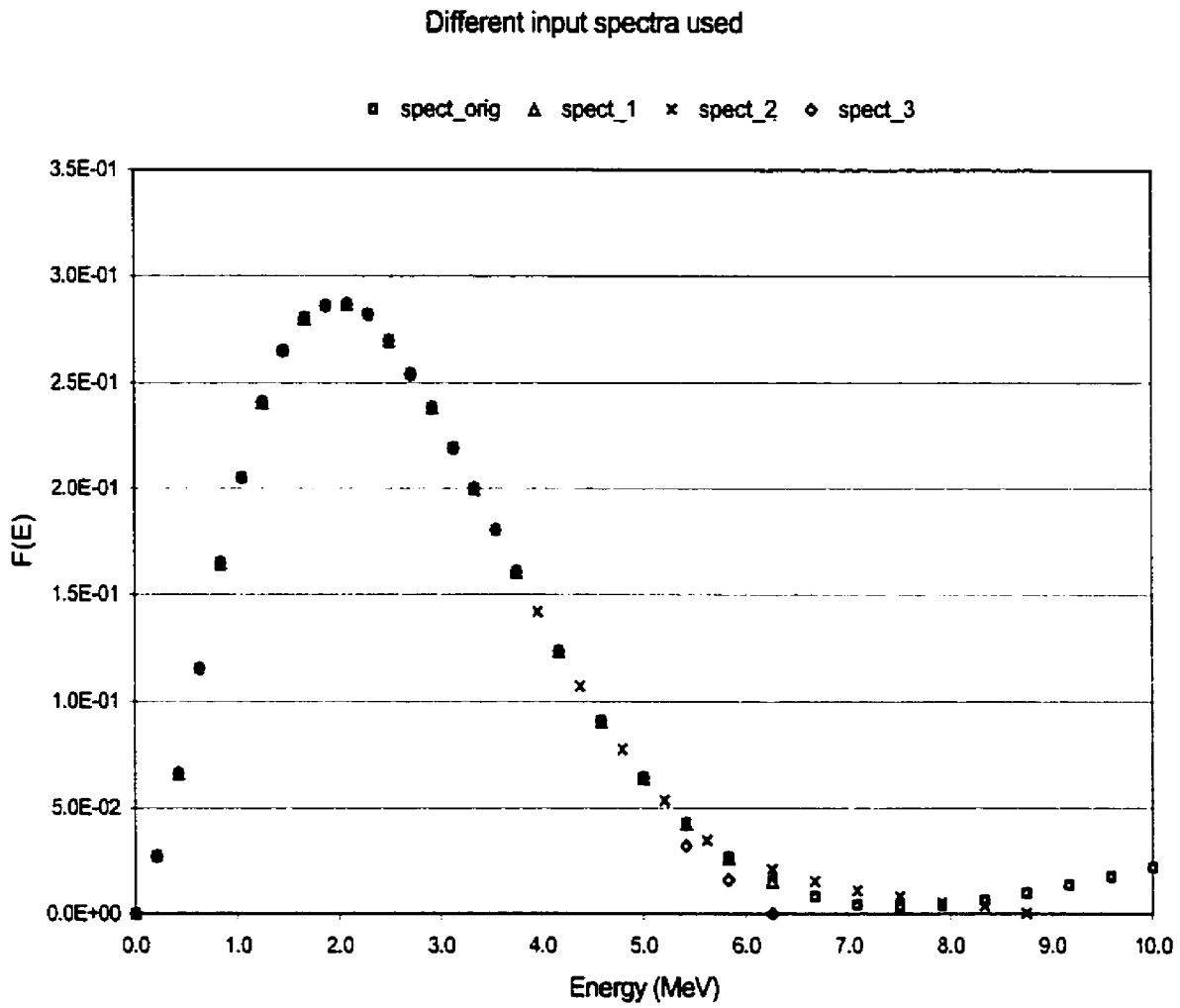
Different input spectra used
spect_orig
spect_1
spect_2
spect_3
3.5E-01
3.0E-01
2.5E-01
2.0E-01
1.5E-01
1.0E-01
5.0E-02
0.0E+00
F(E)
0.0
1.0
2.0
3.0
4.0
5.0
6.0
7.0
8.0
9.0
10.0
Energy (MeV)

Figure 5.1

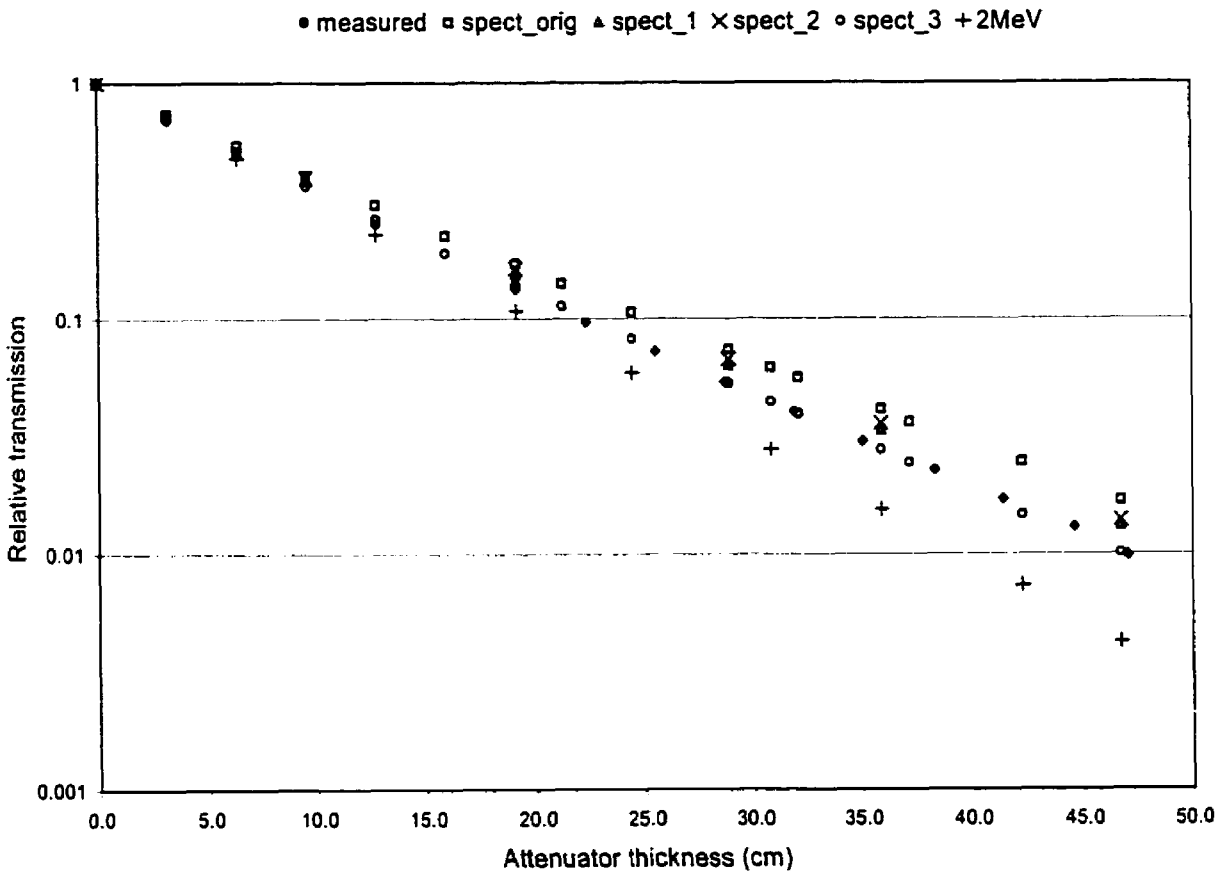
Aluminum attenuator, 1x1 field size
• measured ▫ spect_orig ▲ spect_1 × spect_2 ○ spect_3 + 2MeV
Relative transmission
1
0.1
0.01
0.001
0.0
5.0
10.0
15.0
20.0
25.0
30.0
35.0
40.0
45.0
50.0
Attenuator thickness (cm)

Figure 5.2

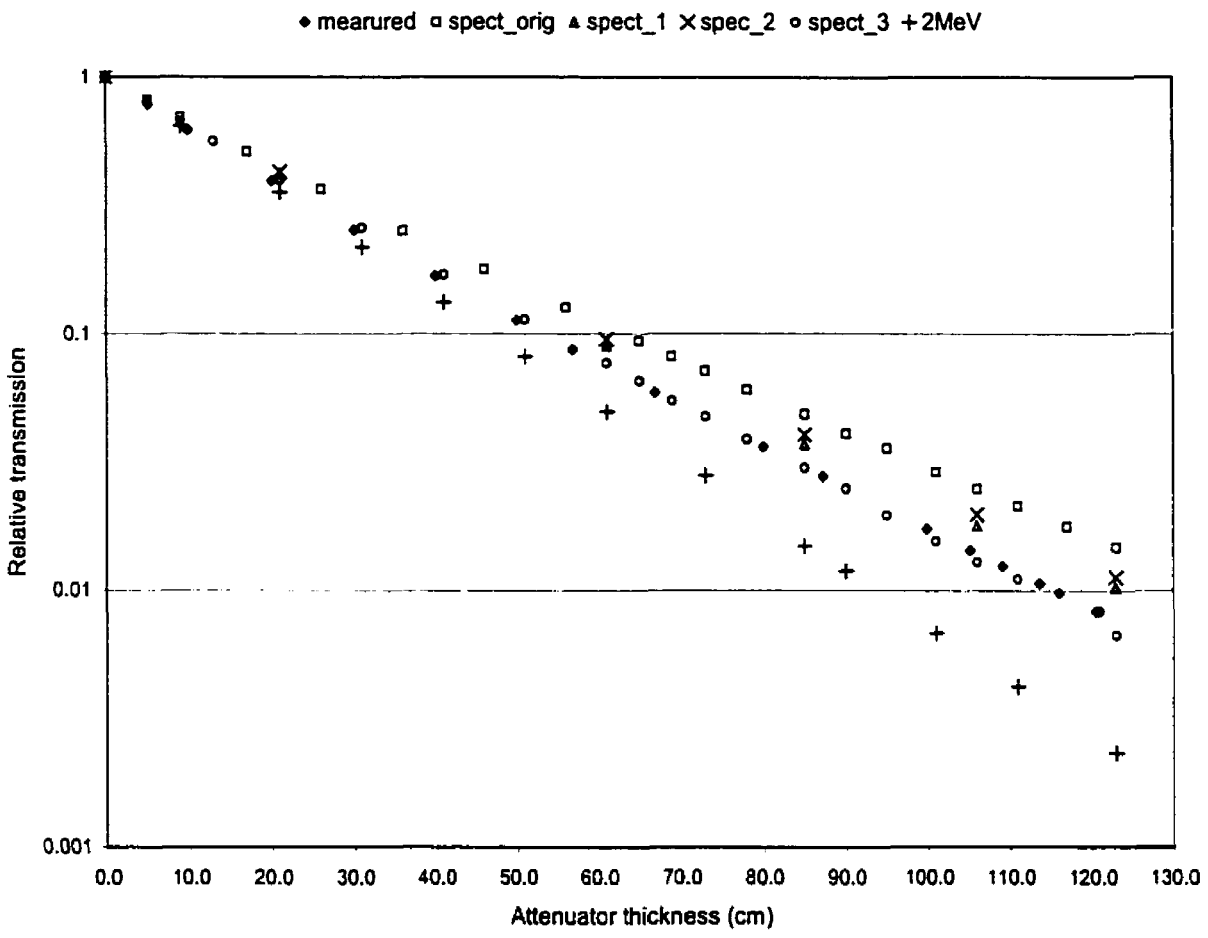
Water attenuator, 1x1 field
◆ mearured ▫ spect_orig ▲ spect_1 × spec_2 ○ spect_3 + 2MeV
Relative transmission
1
0.1
0.01
0.001
0.0
10.0
20.0
30.0
40.0
50.0
60.0
70.0
80.0
90.0
100.0
110.0
120.0
130.0
Attenuator thickness (cm)

Figure 5.3

4.3 Conclusions and Future Work

The purpose of this thesis was to determine the amount of error introduced into the transmission measurements due to the detection of scatter.

The conclusion from the simulations is that there is no significant scatter reaching the detector. In any of the simulated conditions (changing field sizes, source to surface distances, etc.) the scatter contribution to the detected energy was less than 1%, which does not affect the transmission. For the ideal simulation, using the 1x1 field and the detector placed at 330cm from the source, the scatter contribution was less than 0.1%. This is a very important result, taking in consideration that the transmission measurements in narrow beam geometry are widely used.

It was observed that the simulated transmission is very dependent on the input spectrum used. In order to match the simulated transmission with the measured one, various input spectra were tested as described above.

The user code developed (see Appendix A) is a great tool for future simulations of the treatment room or measurements evaluating various geometries.

The results of the actual simulations, the phase-space files, can be used as input files for the simulation of the various ion chambers in order to calculate ion chamber response.

BIBLIOGRAPHY

Attix, F.H. "Introduction to Radiological Physics and Radiation Dosimetry. John Wiley & Sons Inc., 1986 USA

Bielajew, A.F. "Ionization cavity theory: a formal derivation of perturbation factors for thick-walled ion chambers in photon beams" *Phys. Med. Biol.*, Vol. 31, No. 2, 161-170, (1986)

Catala, P. Francois, J. Bonnet, and Ch. Scourarnec. "Reconstruction of 12 MV bremmstrahlung spectra from measured transmission data by direct resolution of the numeric system AF=T" *Medical Physics*. 22(1) January (1995).

Catala, P. Francois. "Simulation of x-ray spectral reconstruction from transmission data by direct resolution of the numeric system AF = T". *Medical Physics*. 20(6) Nov/Dec (1993).

Chaney, E.L., Cullip, T.J., Gabriel, T.A. " A Monte Carlo study of accelerator scatter" *Medical Physics* 21(9), Sept. (1994)

Cook, A.J. "Mortran3 User's Guide" SLAC, Stanford, California (1982)

Duane, S., Bielajew, A.F. and Rogers, D.O.R. "Use of ICRU-37/NBS Collision Stopping Powers in EGS4 System" National Research Council of Canada Rep. PIRS-0173, 1989 – collision stopping powers

Evans, R.D. "The Atomic Nucleus" McGraw-Hill, inc. USA, 1955

Gray, L.H. "An ionization method for the absolute measurement of gamma-ray energy" F.R.S. April (1936)

Hammersley, J.M. and Handscomb D.C. "Monte Carlo meathods" Fletcher & Son Ltd, Norwich, GB, (1964)

Huang P.H., Kenneth R. Kase, and Bengt E. Bjarngard. "Reconstruction of 4-MV bremmstrahlung spectra from measured transmission data" *Medical Physics*. 10(6), Nov/Dec 1983

Hubbell, J.H. "Review of photon interaction cross section data in the medical and biological context" *Phys. Med. Biol.* 44 (1999)

International Commission on Radiation Units and Measurements. "Stopping Powers for Electrons and Positrons" ICRU Rep. 37, 1984 – collision stopping powers

Johns, H.E. and Cunningham, J.R "The physics of radiology", Charles C. Thomas, Illinois, USA, 1983, Fourth Edition

Khan, F.M. "The physics of radiation therapy". Williams & Wilkins, Baltimore, Maryland, USA, 1994, First Edition

Liodofsky, L. Mohan, R. Chui, C. " Energy and angular distribution of photons from medical linear accelerators" *Medical Physics* 12(5), Sept/Oct (1985)

Nelson, W.R., Jenkins, T.M., Rindi, A. "Monte Carlo Transport of Electrons and Photons" *Plenum Press* (1988)

Nisbet, A.et al "Spectral reconstruction of clinical megavoltage photon beams and implications of spectral determinations on the dosimetry of such beams" *Phys. Med. Biol.*, Vol.43, 1507-1521, (1998)

Rogers, D.O. "How accurately can EGS4/PRESTA calculate ion-chamber response?" *Medical Physics* 20(2), Pt.1, Mar/Apr (1993)

Rogers, D.O., Duane, S, Bielajew, A.F., Nelson, W.R. "Use of ICRU-37/NBS Radiative Stopping Powers in the EGS4 System" National Research Council of Canada Rep. PIRS-0177, 1989 – bremsstrahlung cross-sections

Sawchuk, S. "Improved Precision To Photon Energy Spectrum Reconstruction Algorithm" *Medical Physics.* Aug. 1998 WIP-T43

Seltzer, S.M. and Berger, M.J. "Bremsstrahlung Spectra from Electron Interactions with Screened Atomic Nuclei and Orbital Electrons", Nuclear Instrumentation Methods B12, 95-134, 1985 – bremsstrahlung cross-sections

APPENDIX A: User code SCATTEN

```
%N
REPLACE {$MXDATA} WITH {1}  "TO GET OVER NRCCAUX.MOR
DEFINITION"
%L
%C80
!INDENT M 4;
!INDENT F 4;
"*****************************************************************************"
"                                                                             "
"          SCATTEN1.MOR                                                       "
"          ============                                                       "
" XYZDOS MODIFYIED BY GB:                                                    "
"     -SAMPLING FROM A SPECTRUM              GB or SASchuk                  "
"   -DIVERGENT BEAM                          GB                             "
"   -LATCH PARAMETER TO TRACK PARTICLES      GB-TAGS                        "
"   -RANMAR AS A PSEUDO-RANDOM NUMBER GENERATOR                             "
" This code transports photons through attenuator scoring the primary       "
" and scattered transmitted radiation to phase space files, recording       "
" the characteristic information for each particle.  The particles are      "
" going to be discarded at user's request when they reach the region of     "
" interest.  The phase space files will be used as source files for the     "
" detector which is simulated using DOSRZnrc.                               "
"                                                                           "
" Every voxel (volume element) can have different                           "
" materials and/or varying densities (for use with CT data)                 "
"                                                                           "
" A divergent beam of photons is incident on the X-Y surface                "
" perpendicular to the surface.                                             "
```

```
"                                                                    "
"  The geometry is a rectilinear volume with the origin at the       "
"  bottom left, the X-Y plane on the page, X-up, Y to right and the  "
"  Z-axis into the page. Voxel dimensions are completely variable in "
"  all three directions.                                             "
"                                                                    "
"  voxels are labeled by indicies (I,J,K) and defined by:            "
"      XBOUND(I) <= X < XBOUND(I+1)    I <= IMAX                     "
"      YBOUND(J) <= Y < YBOUND(J+1)    J <= JMAX                     "
"      ZBOUND(K) <= Z < ZBOUND(K+1)    K <= KMAX                     "
"                                                                    "
" Unit Assignments                                                   "
" ================                                                  "
"   Unit 1   Output summary and results                              "
"   Unit 5   Input stream - file or terminal                         "
"   Unit 6   prompts for and echoes input                            "
"   Unit 8   echoes input cross-section data (assign a null file)    "
"   Unit 12  input cross section file from PEGS4                     "
"   Unit 20  output file                                             "
"                                                                    "
"  INPUT FILE                                                        "
"  ==========                                                        "
;
" Record 1   TITLE    up to 80 characters                           "
;
" Record 2   NMED     number of media in problem - defaults to 1    "
;
" Record 3(NMED times)  media names, left justified. Note that      "
"                entire volume is initially set to medium 1        "
;
```

```
" Record 4   ECUT,PCUT,ESTEPE(1 TO NMED)                              "
"              electron (total) and photon global cutoff              "
"              energies in MeV                                        "
"              ESTEPE for each medium in the problem                  "
;
" Record 5   IMAX, JMAX, KMAX   3I10                                  "
"              number of voxels in the X,Y,Z directions               "
"              - if <0, it means that number of equally spaced        "
"              boundaries will be input                               "
%E
" Record 6 et seq, repeated for X, Y and Z directions separately      "
"              i.e. repeat the following replacing (I and X) by       "
"              (J and Y) and (K and Z) respectively.                  "
"  if IMAX > 0                                                        "
"          input, one per line, the IMAX + 1  X boundaries            "
"                                                                     "
"  if IMAX < 0                                                        "
"          input smallest X boundary, followed by  ABS(IMAX) pairs    "
"          one pr/line: voxel width, # voxels with this width         "
"                                                                     "
"   for example: starting at record 5                                 "
"          -1,-1,-1                                                   "
"          0.0                                                        "
"          1.0,16                                                     "
"          0.0                                                        "
"          1.0,16                                                     "
"          0.0                                                        "
"          1.0,16                                                     "
"   defines a 16x16x16 cube of 1cm**3 voxels with a total of 4097 reg "
"  or                                                                 "
```

```
"       -1,-1,3                                                    "
"       0.0                                                        "
"       1.0,16                                                     "
"       0.0                                                        "
"       1.0,16                                                     "
"       0.0                                                        "
"       5.0                                                        "
"       10.0                                                       "
"   defines a 16x16x10 cube with 1x1x5 cm voxels stacked 2 deep    "
;
" Record 7 et seg                                                  "
"       IL,IU, JL,JU, KL,KU, MEDIUM, DENSITY 7I10,F10.0            "
"       line is repeated until a blank line found                  "
"       All regions default to medium 1 with its default density   "
"       unless changed here.                                       "
"       For all voxels with                                        "
"            IL <= I <= IU                                         "
"            JL <= J <= JU                                         "
"            KL <= K <= KU                                         "
"       the medium used is MEDIUM and the density used is          "
"       DENSITY. If DENSITY=0.0, the default value for that        "
"       medium is used (faster than entering default density here) "
"       If IU and IL are non-zero, the rest default to all J,K     "
;
" Record 8 et seq                                                  "
"       IL,IU, JL,JU, KL,KU,IZSCAN                                 "
"         as above except these are the regions for which the      "
"         dose will be output. - beware of a paper explosion       "
"        IZSCAN non-zero to get z-scan per page, otherwise         "
"         output is an x-scan per page                             "
```

```
"                                                                    "
;
"  Record 9   XLOWER, XUPPER                                        "
"         boundaries of beam in X direction, in cm                   "
"         -if XLOWER is zero, a value near middle is taken           "
"        If XUPPER is zero, no extent in X direction                 "
;
"  Record 10  YLOWER,YUPPER                                         "
"         as for X direction                                         "
;
%E
"  Record 11    THETAZ,THETAX,THETAY                                "
"        THETAZ: angle of  beam to Z axis (0 is normal)  in degrees  "
"         if THETAZ is zero, others assumed normal(i.e.90 deg)       "
"         If THETAZ is non-zero - and others both are zero, THETAX is "
"                          as large as possible - i.e. max cos       "
"                          allowed, and THETAY is 90 deg             "
"                        - if THETAX is non-zero, it may be          "
"                          reduced if too large, and THETAY          "
"                          will be choosen to normalize the          "
"                          direction cosines                         "
"  note: see NRCC code INHOM for examples of more complex incident beams "
;
"  Record 12                                                         "
"         EIN, IQIN, NCASE, IWATCH, TIMMAX, INSEED                   "
"         EIN    kinetic energy of incident beam in MeV              "
"         IQIN   charge of incident beam                             "
"         NCASE  # histories                                         "
"         IWATCH =0, no tracking output, 1 all interaction,2 all steps "
"         TIMMAX   not used                                          "
```

```
"        INSEED   input random # seed  (0  is OK)                              "
"                                                                               "
"  Version 1   March 1986   D.W.O.Rogers, NRCC Ottawa                          "
"  Version 1.1 Aug   1989   A F Bielajew, NRCC Ottawa                          "
"                        -Coded Machine Independent Version                     "
"             Oct 1993     DWOR corrected error-amass had assumed             "
"                        unit density prior to this                             "
"             Dec 1996     DWOR made minor change in stmt order    in         "
"                        HOWFAR so compiles on Linux                            "
"*******************************************************************************"


"STEP 1  USER OVERRIDES AND DECLARATIONS"
"============================================================="
"%U8  PICK UP NRCC MACROS                                                      "
%L    "TURN ON LISTING AGAIN                                                   "
REPLACE {$MXMED} WITH {4}
REPLACE {$MXREG} WITH {8416}
REPLACE {$MXSTACK} WITH {20}
REPLACE {$IMAX} WITH {17}
REPLACE {$JMAX} WITH {15}
REPLACE {$KMAX} WITH {33}     "X,Y,Z GRID MAXIMA                               "
REPLACE {$STAT} WITH {10}   "USE 10 BATCHES IN CALCULATIONS"
REPLACE {$ITMAX} WITH {1}
REPLACE {$MXDOS} WITH {5}     "MAX NUMBER OF GROUPS OF                         "
" REGIONS TO ANALYSE                                                           "

"  SOME MACROS FOR FACILITATING ACCESS TO BOUNDARIES                           "
" AND REGIONS                                                                  "
REPLACE {$GETIR(#,#,#)} WITH {1 + {P1} + ({P2}-1)*IMAX + ({P3}-1)*IJMAX}
```

```
REPLACE {;$DECODEIR(#,#,#,#);} WITH
"FIRST PARAMETER IS INPUT REGION, NEXT 3 ARE DECODED I,J,K      "
{;{P2}=MOD({P1}-1,IMAX);  IF({P2} = 0)[{P2}=IMAX;]
{P4} = 1 + ({P1}-1-{P2})/IJMAX;
{P3} = 1 + ({P1}-1-{P2} - ({P4}-1)*IJMAX)/IMAX;}

REPLACE {;COMIN/GEOM/;} WITH
"      ============="
{;COMMON/GEOM/XBOUND($IMAX+1),YBOUND($JMAX+1),ZBOUND($KMAX
+1),
IMAX,JMAX,KMAX,IJMAX,IRMAX,IRS1,ISL1,ISU1,JSL1,JSU1,KSL1,KSU1,
IRS2,ISL2,ISU2,JSL2,JSU2,KSL2,KSU2,
IRS3,ISL3,ISU3,JSL3,JSU3,KSL3,KSU3,IRS4,ISL4,ISU4,JSL4,JSU4,KSL4,KSU
4;}
"  IMAX,JMAX,ZMAX   MAXIMUM NUMBER OF CELLS IN X,Y,Z DIRECTION
FOR  "
"              THIS PROBLEM"
"  IJMAX  NUMBER OF CELLS IN X-Y PLANE = IMAX*JMAX                "
"  IRMAX  MAXIMUM NUMBER OF REGIONS =KMAX*IJMAX + 1          "
%E
REPLACE {;OUTPUT61#;#;} WITH
"     ==============          GENERALIZED OUTPUT TO UNITS 6 AND 1 "
{;{SETR A =@LG}
WRITE(6,{COPY A}){P1};WRITE(1,{COPY A}){P1};{COPY A}FORMAT{P2};}

;
REPLACE {;COMIN/SCORE/;} WITH
"      =============="
{;COMMON/SCORE/IWATCH,IS,MXNP,SNPRIME($STAT),
```

```
SNBREM($STAT),SNCOMPT($STAT),SNANNIH($STAT),SEPRIME($STAT),
SEBREM($STAT),SECOMPT($STAT),SEANNIH($STAT),SNCHPART($STAT),
SECHPART($STAT),
UNPRIME,UNBREM,UNCOMPT,UNANNIH,UEPRIME,UEBREM,UECOMPT,UE
ANNIH,
UNCHPART,UECHPART;}

"AUSGAB will count the number of transmitted primaries, bremsstrahlung "
"Compton scattered and positron annihilation photons, and possible      "
"charged particles which would hit the detector area.                   "
;
"The following two macros are added to the code in the process of tag   "
REPLACE {;COMIN/STACK/;} WITH
{;COMMON/STACK/$LGN(E,X,Y,Z,U,V,W,DNEAR,WT,IQ,IR,LATCH($MXSTAC
K)),
LASTIR($MXSTACK),LATCHI,NP;}
"Note this macro adds the variable array LATCH and its initial          "
"value LATCHI to be common stack in every routine.  The values of       "
"LATCH are passed to all succeeding generations of particles.           "
;
REPLACE {TRANSFER PROPERTIES TO # FROM #;} WITH
{X{P1}=X{P2};Y{P1}=Y{P2};Z{P1}=Z{P2};IR{P1}=IR{P2};WT{P1}=WT{P2};
DNEAR{P1}=DNEAR{P2};LATCH{P1}=LATCH{P2};}
"                GB-TAGS 30/03/2000                                     "

;
"RANDOM VARIABLE COMMON                                                 "
"RANDM0, RANNDM1, RANDM2 ARE SHADOW AREAS USED FOR                      "
"CORRELATIONS                                                           "
REPLACE {;COMIN/RANDOM/;} WITH {;
```

```
COMMON/RANDOM/URNDM(97),CRNDM,CDRNDM,CMRNDM,IXX,  JXX  ;
COMMON/RANDM0/UDM0(97), CDM0, CDDM0, CMDM0, IXXDM0,JXXDM0;
COMMON/RANDM1/UDM1(97), CDM1, CDDM1, CMDM1, IXXDM1,JXXDM1;
COMMON/RANDM2/UDM2(97), CDM2, CDDM2, CMDM2, IXXDM2,JXXDM2;
}
;
REPLACE {$RNG-INITIALIZATION;} WITH {;
 CALL RMARIN;
}
;
REPLACE {$STORE-RNG(#);} WITH {;
 IF({P1}.EQ.0)[
    DO I=1,97[UDM0(I)=URNDM(I);]

CDM0=CRNDM;CDDM0=CDRNDM;CMDM0=CMRNDM;IXXDM0=IXX;JXXDM0=
JXX;
    ]
 ELSEIF({P1}.EQ.-1)[
    DO I=1,97[UDM1(I)=URNDM(I);]

CDM1=CRNDM;CDDM1=CDRNDM;CMDM1=CMRNDM;IXXDM1=IXX;JXXDM1=
JXX;
    ]
 ELSEIF({P1}.EQ.-2)[
    DO I=1,97[UDM2(I)=URNDM(I);]

CDM2=CRNDM;CDDM2=CDRNDM;CMDM2=CMRNDM;IXXDM2=IXX;JXXDM2=
JXX;
    ]
 ELSE[
```

```
    WRITE({P1},*)URNDM,CRNDM,CDRNDM,CMRNDM,IXX,JXX;
    ]
}
;
REPLACE {$RESET-RNG(#);} WITH {;
 IF({P1}.EQ.0)[
    DO I=1,97[URNDM(I)=UDM0(I);]

CRNDM=CDM0;CDRNDM=CDDM0;CMRNDM=CMDM0;IXX=IXXDM0;JXX=JXX
DM0;
    ]
 ELSEIF({P1}.EQ.-1)[
    DO I=1,97[URNDM(I)=UDM1(I);]

CRNDM=CDM1;CDRNDM=CDDM1;CMRNDM=CMDM1;IXX=IXXDM1;JXX=JXX
DM1;
    ]
 ELSEIF({P1}.EQ.-2)[
    DO I=1,97[URNDM(I)=UDM2(I);]

CRNDM=CDM2;CDRNDM=CDDM2;CMRNDM=CMDM2;IXX=IXXDM2;JXX=JXX
DM2;
    ]
 ELSE[
    READ({P1},*)URNDM,CRNDM,CDRNDM,CMRNDM,IXX,JXX;
    ]
}

;
REPLACE {$COMMON-RANDOM-DECLARATION-IN-BLOCK-DATA;} WITH {;
```

```
 ;COMIN/RANDOM/;
}

;
REPLACE {$RANDOMSET#;} WITH {
   {P1}=URNDM(IXX)-URNDM(JXX); IF({P1}.LT.0.) {P1}={P1}+1.; URNDM(IXX)
= {P1};
   IXX=IXX-1; IF(IXX.EQ.0) IXX=97;
   JXX=JXX-1; IF(JXX.EQ.0) JXX=97;
   CRNDM=CRNDM-CDRNDM; IF(CRNDM.LT.0.) CRNDM=CRNDM+CMRNDM;
   {P1}={P1}-CRNDM; IF({P1}.LT.0.) {P1}={P1}+1.;
}
        "GB-TAGS 30/03/2000"
;
;COMIN/BOUNDS,EPCONT,GEOM,MEDIA,MISC,RANDOM,SCORE,STACK,T
HRESH/;

"INTEGER ISL,ISU,JSL,JSU,KSL,KSU;"
;
REAL AMASS($IMAX,$JMAX,$KMAX),ESTEPE($MXMED);
;
" GB 25/02/2000, SASawchuk                                          "
;
" For Spectrum Sampling                                             "
;
REAL RANDNO,F(25),FBRANCH(26),EBIN(25),FSAMP(25),ENBIN,FBR(25);
"                                                                   "
CHARACTER TITLE(80);

$DECLARE_TIMING_VARIABLES;
```

```
$INITIALIZE_IO;
$INITIALIZE_ELAPSED_CPU_TIME;
OUTPUT61;(///'1',T20,'NRCC USER CODE XYZDOS(V01)  USING EGS4'//
' GEOMETRY IS A RECTILINEAR VOLUME, ORIGIN IN BOTTOM LEFT,X-Y
PLANE ON'/T20,
'THE PAGE AND Z AXIS INTO THE PAGE'//);
OPEN(20,FILE='AL.OUT',STATUS='UNKNOWN');
OUTPUT61;(8x,71('-')/'$TITLE: ');INPUT TITLE;(80A1);
OUTPUT61 TITLE;('+',3X,80A1/8X,71('-'));


"STEP 2  PRE-HATCH CALL INITIALIZATION"
"====================================="

OUTPUT61;('$NUMBER OF MEDIA: ');READ(5,*) NMED;
IF(NMED=0 | NMED>$MXMED) [NMED= 1;"DEFAULTS TO 1 MEDIUM"]
OUTPUT61 NMED;('+',T10,I7);

DO N=1,NMED[
OUTPUT61 N;('$MEDIUM',I3,':  ');INPUT (MEDIA(J,N),J=1,24);(24A1);
OUTPUT61 (MEDIA(J,N),J=1,24);('+',T20,24A1);]

DO N=2,$MXREG [MED(N)=1;] "I.E. EVERYTHING THE FIRST MEDIUM "
" CAN BE CHANGED BELOW ON A REGION BY REGION BASIS          "

OUTPUT61 NMED;('$ECUT,PCUT,ESTEPE(1 to',I2,'):  ');
READ(5,*) ECUTIN,PCUTIN,(ESTEPE(I),I=1,NMED);
OUTPUT61 ECUTIN,PCUTIN,(ESTEPE(I),I=1,NMED);('+',T10,12F10.3);
DO N=2,$MXREG[ECUT(N)=ECUTIN;PCUT(N)=PCUTIN;]
$RNG-INITIALIZATION;
```

```
          "GB-TAGS 30/03/2000"
"STEP 3    HATCH CALL"
"====================="

"WE DO THIS JUST BEFORE STEP 7 SO CAN CHECK ALL INPUTS FIRST"

%E
"STEP 4   INITIALIZATION FOR HOWFAR"
"================================="

"    INPUT X, Y, Z BOUNDARIES                                    "
"                                                                "

"FIRST DEFINE A MACRO WHICH WILL BE USED FOR EACH AXIS IN TURN"
REPLACE {$GET-#-BOUNDARIES;} WITH {
;IF(MAX{P1} > 0) ["JUST PICK UP BOUNDARIES ONE AT A TIME         "
   DO I=1,MAX{P1}[
      OUTPUT61 I;('$SMALL BOUNDARY FOR REGION(',I3,')  ');
      READ(5,*) {P1}BOUND(I);
      IF(I ~=1 & {P1}BOUND(I)<={P1}BOUND(I-1))[
         OUTPUT61;(' BOUNDARY OUT OF ORDER**************');]
      OUTPUT61 {P1}BOUND(I);('+',T10,F12.3);
      ]
   OUTPUT61 MAX{P1};('$OUTER BOUNDARY FOR REGION(',I3,')  ');
   READ(5,*) {P1}BOUND(MAX{P1} + 1);
   OUTPUT61 {P1}BOUND(MAX{P1}+1);('+',T10,F12.3);
   ]
ELSE ["MAX(P1) < 0, INPUT GROUPS OF REGIONS                      "
   "ASSUME MAXBD SET TO $IMAX,$JMAX OR $KMAX                     "
   OUTPUT61;('$INITIAL BOUNDARY: ');READ(5,*) {P1}BOUND(1);
```

```
   OUTPUT61 {P1}BOUND(1);('+',F12.3);
   NGROUP = - MAX{P1};  "NO. OF GROUPS IN THIS DIRECTION        "
   MAX{P1} = 0;
   DO IGROUP = 1,NGROUP[
      OUTPUT61;('$WIDTH IN THIS GROUP, NO. OF REGIONS IN GROUP:
');
      READ(5,*) WIDTH,NN;
      IF(NN<=0) [NN=1;] IF(WIDTH<=0.0)[WIDTH=1.0;]
      OUTPUT61 WIDTH,NN;('+',F12.3,I5);
      NNN = MIN(NN,MAXBD-MAX{P1});"ENSURE DONT ADD TOO MANY"
"REGIONS                                                    "
      IF(NNN ~= 0)[
         DO IN = MAX{P1}+1, MAX{P1}+NNN [
            {P1}BOUND(IN+1) = {P1}BOUND(IN)+WIDTH;]]
     IF(NN ~= NNN) [OUTPUT;(T15,'***NO. REGIONS REDUCED***'/);]
   MAX{P1} = MAX{P1}+NNN;]
"MUST SET IMAX ETC AFTER CALL TO THIS MACRO"
OUTPUT61 ({P1}BOUND(I),I=1,MAX{P1}+1);(' BOUNDARIES'/(6F12.3));
   ]"END OF ELSE"
}


;OUTPUT61;(/'$# REGIONS IN X,Y,Z DIRECTIONS (IF<0,IMPLIES # GROUPS
OF REG): ');
READ(5,*) MAXX,MAXY,MAXZ;

IF(MAXX = 0) MAXX=1;  IF(MAXX>$IMAX)MAXX=$IMAX;
IF(MAXY = 0) MAXY=1;  IF(MAXY>$JMAX)MAXY=$JMAX;
IF(MAXZ = 0) MAXZ=1;  IF(MAXZ>$KMAX)MAXZ=$KMAX;
OUTPUT61 MAXX,MAXY,MAXZ;('+',3I6);
```

```
MAXBD=$IMAX;OUTPUT61;(/T20,'INPUT BOUNDARIES IN THE X
DIRECTION');
$GET-X-BOUNDARIES; IMAX=MAXX;
MAXBD=$JMAX;OUTPUT61;(/T20,'INPUT BOUNDARIES IN THE Y
DIRECTION');
$GET-Y-BOUNDARIES; JMAX=MAXY;
MAXBD=$KMAX;OUTPUT61;(/T20,'INPUT BOUNDARIES IN THE Z
DIRECTION');
$GET-Z-BOUNDARIES; KMAX=MAXZ;

IJMAX = IMAX*JMAX;  IRMAX =1 + IMAX*JMAX*KMAX;
%E
OUTPUT61 IRMAX;('0TOTAL # REGIONS INCLUDING EXTERIOR =',I5);
IF(IRMAX > $MXREG)[OUTPUT61;('0****THATS TOO MANY
REGIONS*****'//);STOP;]
"  GET DENSITY OR MATERIAL FOR EACH REGION                    "
"  RHOR = 0.0 MEANS USE DEFAULT DENSITY FOR THE MATERIAL IN"
"REGION"

OUTPUT61;('0INPUT GROUPS OF REGIONS FOR WHICH DENSITY AND
MEDIUM ARE',
' NOT DEFAULTS');
LOOP [ OUTPUT61;('$LOWER,UPPER I, J, K,  MEDIUM, DENSITY');
READ(5,*) IL,IU,JL,JU,KL,KU,MEDTMP,RHOTMP;
IF( IL = 0 & IU = 0)["BLANK LINE, SO QUIT" EXIT;]
"CHECK IL ETC ARE OK"
IF(IL <= 0) IL = 1; IF(IU <= 0 | IU >= IMAX)[IU = IMAX;]
IF(JL <= 0) JL = 1; IF(JU <= 0 | JU >= JMAX)[JU = JMAX;]
IF(KL <= 0) KL = 1; IF(KU <= 0 | KU >= KMAX)[KU = KMAX;]
```

```
IF(MEDTMP < 0 | MEDTMP > NMED)[MEDTMP = 1;]
OUTPUT61 IL,IU,JL,JU,KL,KU,MEDTMP,RHOTMP;('+',3('(',I3,I4,')'), I4, F10.3);

DO I=IL,IU [ DO J=JL,JU [ DO K=KL,KU[
IRL = 1 + I +(J-1)*IMAX + (K-1)*IJMAX;
 RHOR(IRL)=RHOTMP;  MED(IRL)=MEDTMP; ]]]
]"END OF LOOP ON GROUPS OF REGIONS"


"STEP 5  INITIALIZATION FOR AUSGAB"
"================================="

/IAUSFL(8),IAUSFL(19),IAUSFL(14),IAUSFL(15)/=1;
READ(5,*) ISL1,ISU1,JSL1,JSU1,KSL1,KSU1;
OUTPUT61;('0ISL1,ISU1,JSL1,JSU1,KSL1,KSU1 ');
OUTPUT61 ISL1,ISU1,JSL1,JSU1,KSL1,KSU1;('+',T5,6I8);
IF(ISL1<=0)ISL1=1;
IF(ISU1<=0 |ISU1>=IMAX) ISU1=IMAX;
IF(JSL1<=0)JSL1=1;
IF(JSU1<=0 |JSU1>=JMAX) JSU1=JMAX;
IF(KSL1<=0)KSL1=1;
IF(KSU1=0 |KSU1>=KMAX) KSU1=KMAX;
IRS1=(1+(ISL1)+((JSL1)-1)*IMAX+((KSL1)-1)*IJMAX);
OUTPUT61;('0IRS1 ');
OUTPUT61 IRS1;('+',T5,I8);
;
READ(5,*) ISL2,ISU2,JSL2,JSU2,KSL2,KSU2;
OUTPUT61;('0ISL2,ISU2,JSL2,JSU2,KSL2,KSU2 ');
OUTPUT61 ISL2,ISU2,JSL2,JSU2,KSL2,KSU2;('+',T5,6I8);
IF(ISL2<=0)ISL2=1;
```

```
IF(ISU2<=0 |ISU2>=IMAX) ISU2=IMAX;
IF(JSL2<=0)JSL2=1;
IF(JSU2<=0 |JSU2>=JMAX) JSU2=JMAX;
IF(KSL2<=0)KSL2=1;
IF(KSU2=0 |KSU2>=KMAX) KSU2=KMAX;
IRS2=(1+(ISL2)+((JSL2)-1)*IMAX+((KSL2)-1)*IJMAX);
OUTPUT61;('0IRS2 ');
OUTPUT61 IRS2;('+',T5,I8);
;
READ(5,*) ISL3,ISU3,JSL3,JSU3,KSL3,KSU3;
OUTPUT61;('0ISL3,ISU3,JSL3,JSU3,KSL3,KSU3 ');
OUTPUT61 ISL3,ISU3,JSL3,JSU3,KSL3,KSU3;('+',T5,6I8);
IF(ISL3<=0)ISL3=1;
IF(ISU3<=0 |ISU3>=IMAX) ISU3=IMAX;
IF(JSL3<=0)JSL3=1;
IF(JSU3<=0 |JSU3>=JMAX) JSU3=JMAX;
IF(KSL3<=0)KSL3=1;
IF(KSU3=0 |KSU3>=KMAX) KSU3=KMAX;
IRS3=(1+(ISL3)+((JSL3)-1)*IMAX+((KSL3)-1)*IJMAX);
OUTPUT61;('0IRS3 ');
OUTPUT61 IRS3;('+',T5,I8);
;
READ(5,*) ISL4,ISU4,JSL4,JSU4,KSL4,KSU4;
OUTPUT61;('0ISL4,ISU4,JSL4,JSU4,KSL4,KSU4 ');
OUTPUT61 ISL4,ISU4,JSL4,JSU4,KSL4,KSU4;('+',T5,6I8);
IF(ISL4<=0)ISL4=1;
IF(ISU4<=0 |ISU4>=IMAX) ISU4=IMAX;
IF(JSL4<=0)JSL4=1;
IF(JSU4<=0 |JSU4>=JMAX) JSU4=JMAX;
IF(KSL4<=0)KSL4=1;
```

```
IF(KSU4=0 |KSU4>=KMAX) KSU4=KMAX;
IRS4=(1+(ISL4)+((JSL4)-1)*IMAX+((KSL4)-1)*IJMAX);
OUTPUT61;('0IRS4 ');
OUTPUT61 IRS4;('+',T5,I8);
;
"STEP 6 DETERMINATION OF INCIDENT PARTICLE PARAMETERS     "
"=========================================================="

"DEFINE SOURCE   -A PARALLEL BEAM INCIDENT ON X-Y SURFACE "

OUTPUT61;(/' SPECIFICATIONS FOR DIVERGENT BEAM, INCIDENT ON X-Y
SURFACE'//
'$INCIDENT ON WHAT RANGE OF X VALUES? ');
READ(5,*)  XINL,XINU;
IF(XINL = 0.0)[XINL = XBOUND(IMAX+1)/2.;"DEFAULT TO NEAR MIDDLE"]
IF(XINL < XBOUND(1))[XINL = XBOUND(1);]
IF(XINU <= XINL)[ XINU = XINL;"DEFAULT A PENCIL BEAM"]
%E
"CHECK NOT TOO BIG"
IF(XINU> XBOUND(IMAX+1)) [XINU=XBOUND(IMAX+1);]
IF(XINL> XBOUND(IMAX+1)) [XINL=XBOUND(IMAX+1);]
OUTPUT61 XINL,XINU;('+',T10,2F10.3);
XINDEL = XINU-XINL;
"NOW SEARCH FOR INITIAL REGION X INDEX RANGE"
IXINL=0;
LOOP[IXINL=IXINL+1;] UNTIL (XBOUND(IXINL) <= XINL & XBOUND(IXINL+1)
> XINL);
IXINU=IXINL-1;
LOOP[IXINU=IXINU+1;] UNTIL (XBOUND(IXINU) <= XINU &
XBOUND(IXINU+1) >= XINU);
```

```
OUTPUT61 IXINL,IXINU;(T40,'X INDEX RANGES OVER I=',I3,' to',I4);

OUTPUT61;('$INCIDENT ON WHAT RANGE OF Y VALUES? ');
READ(5,*)  YINL,YINU;
IF(YINL = 0.0)[YINL = YBOUND(JMAX+1)/2.;"DEFAULT TO NEAR MIDDLE"]
IF(YINL < YBOUND(1)) [YINL = YBOUND(1);]
IF(YINU <= YINL)[ YINU = YINL;"DEFAULT A PENCIL BEAM"]
"CHECK NOT TOO BIG"
IF(YINU> YBOUND(JMAX+1)) [YINU=YBOUND(JMAX+1);]
IF(YINL> YBOUND(JMAX+1)) [YINL=YBOUND(JMAX+1);]
OUTPUT61 YINL,YINU;('+',T10,2F10.3);
YINDEL = YINU-YINL;
"NOW SEARCH FOR INITIAL REGION Y INDEX RANGE"
JYINL=0;
LOOP[JYINL=JYINL+1;] UNTIL (YBOUND(JYINL) <= YINL &
YBOUND(JYINL+1) > YINL);
JYINU=JYINL-1;
LOOP[JYINU=JYINU+1;] UNTIL (YBOUND(JYINU) <= YINU &
YBOUND(JYINU+1) >= YINU);
OUTPUT61 JYINL,JYINU;(T40,'J INDEX RANGES OVER J=',I3,' to',I4);
;
"OUTPUT61;('$ANGLE OF BEAM TO AXES(in deg, 0 IS NORMAL): ');"
"READ(5,*) THETAZ,THETAX,THETAY;"
"WIN = COS(THETAZ*3.141593/180.);"
"UIN = COS(THETAX*3.141593/180.);"
"UIN = MIN (UIN,SQRT(1.0 - WIN**2)); MAKE SURE NOT TOO BIG"
"THETAX = ACOS(UIN)*180./3.141593;"
"VIN = SQRT(1 - WIN**2 - UIN**2+1.E-7);THETAY=ACOS(VIN)*180./3.14159;"
"NOTE WE DONT EVEN USE THE INPUT VALUE OF THETAY"
"OUTPUT61;('$THETAZ,THETAX,THETAY');                "
```

```
"OUTPUT61 THETAZ,THETAX,THETAY;('+ ',3F10.2,' deg');"

"READ(5,*) IQIN,NCASE,IWATCH,TIMMAX,INSEED;   GB-TAGS 31/05/2000"
READ(5,*) IQIN,NCASE,IWATCH,TIMMAX,INSEED,ZIN;   "GB-TAGS
06/07/2000"
;
" Insert Energy Spectra data        "
" GB 25/02/2000, SASawchuk  "
"    Part 1                  "
;
%F
     OPEN(99,FILE='spect.inp',STATUS='UNKNOWN')
C    OPEN(99,FILE='spctsmp.out',STATUS='UNKNOWN')
     READ(99,*)ENBIN
C    write(*,*)ENBIN
C ENERGY LIMITS - MIN AND MAX
C NUMBER OF ENERGY NODES (NUMBER OF BINS + 1)
C READ IN NORMALIZED SPECTRUM VALUES AND CREATE CDF FOR
EACH BRANCHING RATIO
     IN=1
5    CONTINUE
     READ(99,*,END=99)EBIN(IN),F(IN)
     IN=IN+1
     GO TO 5
99   CONTINUE
C GET TOTAL NUMBER OF NODES (NUMBER OF BINS + 1)
C NB THAT ENBINS (NUMBER OF BINS MUST BE ONE LESS THAN M
(NUBER OF NODES)
     M=IN-1
     DO I=1,M
```

```
    FSAMP(I)=0.0
    END DO
C GET BIN SIZE
    E0=EBIN(1)
    EM=EBIN(M)
    DELTAE=(EM-E0)/ENBIN
C Use Trapezoidal Rule to integrate numerically to get CDF FBRANCH
C Simpson's Rule (more accurate) can be used but will require three nodes at
once
    FBRANCH(1)=0.0
C FBR(1) IS THE AREA UNDER THE FIRST BIN USING TRAPEZOIDAL RULE
    FBRANCH(2)=(F(2)+F(1))*DELTAE/2.
    DO J=3,M
    FBR(J)=(F(J-2)+4.0*F(J-1)+F(J))*DELTAE/3.
    ENDDO
    FBRANCH(3)=FBR(3)
    DO J=4,M
    FBRANCH(J)=FBR(J)+FBRANCH(J-2)
    END DO
%M
;
"                              "
" Done part 1 for sampling energy spectra "
"                              "
;
IF(TIMMAX<=0.0)[TIMMAX = 0.99; "DEFAULT 1 HOUR"]
JCASE = NCASE/$STAT; NCASE = JCASE*$STAT;
IF(INSEED ~= 0) [IXX = INSEED;]
"IF(IQIN = 0) [ETOTIN = EIN;] ELSE [ETOTIN = EIN + 0.511;]"
                    "GB-TAGS 31/05/2000"
```

```
;
WTIN=1.0;
"LATCHI = 0;"
ETOTIN=0.0;          "GB-TAGS 26/04/2000"

DO IS=1,$STAT[
/SNPRIME(IS),SNCOMPT(IS),SNBREM(IS),SNANNIH(IS),SNCHPART(IS)/=0;
/SEPRIME(IS),SECOMPT(IS),SEBREM(IS),SEANNIH(IS),SECHPART(IS)/=0.0;]

"DELAYED STEP 3"
"=============="

OUTPUT;(//T20,'CALL HATCH'/);  CALL HATCH;
OUTPUT61;(/' MEDIUM',T25,'AE',T35,'AP');
DO N=1,NMED[
OUTPUT61 (MEDIA(J,N),J=1,15),AE(N),AP(N);(1X,15A1,2F10.3);]
OUTPUT61;(//);

DO I=1,NMED[ CALL FIXTMX(ESTEPE(I),I);] "REDUCE ELECTRON STEPS"

IF(IWATCH ~= 0)[CALL WATCH(-99,IWATCH);]  "SET UP FOR WATCH
ROUTINE IF NEEDED"

"IMPLEMENT PRESTA gb 25/02/2000"
"EK0=EIN;"
"$PRESTA_INPUTS; INPUT THE PRESTA VARIABLES"
"$PRESTA_INPUT_SUMMARY; OUTPUT THE PRESTA INPUT VARIABLES"

%E
"STEP 7   SHOWER CALL"
```

```
"====================="

$SET_ELAPSED_CPUTIME(CPUT0); "OBTAIN THE INITIAL STARTING TIME"
OUTPUT61 CPUT0*$CONVERSION_TO_SECONDS;(' CPUTIME SO
FAR=',F12.3,' s'/);

DO IS = 1,$STAT [ "BREAK INTO $STAT BATCHES"

$SET_ELAPSED_CPUTIME(CPUT1);
TIMCPU=(CPUT1-
CPUT0)*$CONVERSION_TO_SECONDS+$TIME_RESOLUTION;
"CPUTIME ON SIMULATIONS ONLY SO FAR"
OUTPUT IS,TIMCPU,IXX;(' START BATCH',I3,'  CPUTIME=',F10.1,' s
RNG=',I12);
DO IHIST = 1,JCASE[
" GB 25/02/2000, SASAWCHUK          "
" Begin part 2 for sampling energy spectra"
"                                   "
;
$RANDOMSET RANDNO;
;
%F
C    Place within SHOWER Loop
     IF(RANDNO.GT.FBRANCH(M))FSAMP(M)=FSAMP(M)+1.
C     write(*,*)fbranch(m),m,randno
     DO JJ=1,M-1

IF((FBRANCH(JJ).LE.RANDNO).AND.(FBRANCH(JJ+1).GT.RANDNO))THEN
C     FSAMP(JJ)=FSAMP(JJ)+1.0
     EIN=EBIN(JJ)
```

```
      ETOTIN=ETOTIN+EIN
C     WRITE(*,*)EIN,ETOTIN
      GO TO 11
      ENDIF
      END DO
11    CONTINUE
C     DO I=1,M
C     FSAMP(I)=FSAMP(I)/(FLOAT(N)*DELTAE)
C     END DO
C     WRITE(2,*)' '
C     WRITE(2,*)'SPECTRUM AND SAMPLING SPECTRUM'
C     DO I =1,M
C     WRITE(2,*)EBIN(I),F(I),FSAMP(I)
C     IF(I.NE.M)THEN
C     WRITE(3,*)EBIN(I),FSAMP(I)
C     WRITE(3,*)EBIN(I+1),FSAMP(I)
C     ENDIF
C     END DO
C     STOP
C     END
%M
"                              "
" Done part 2 for sampling energy spectra"
"                              "
;
"NEED HERE TO SELECT XIN,YIN,IRIN"
IF(XINDEL = 0.0)[XIN=XINL;I=IXINL;]
ELSE [ $RANDOMSET R1;XIN = XINL + R1*XINDEL;
I=IXINL-1;LOOP[I=I+1;]UNTIL(XBOUND(I)<=XIN & XBOUND(I+1)>XIN);]
IF(YINDEL = 0.0)[YIN=YINL;J=JYINL;]
```

```
ELSE [  $RANDOMSET R1;YIN = YINL + R1*YINDEL;
J=JYINL-1;
LOOP[J=J+1;]UNTIL(YBOUND(J)<=YIN & YBOUND(J+1)>YIN);]
K=1;
IRIN = 1 + I +(J-1)*IMAX;  "INPUT REGION"
"DEFINE A CENTER POINT FOR THE XY-COORDINATES XC AND YC"
XC=XINL+XINDEL/2.;
YC=YINL+YINDEL/2.;

"Input of 1X1 cm divergent beam at SAD=100cm to attenuator          "
"this means 0.75x0.75 cm at the attenuator's surface which is at 75 cm "
"from the source.  WE INPUT ZIN=75.0cm IN THE INPUT- LAST LINE      "
LENGTH=SQRT((XIN-XC)**2+(YIN-YC)**2+ZIN**2);
UIN=(XIN-XC)/LENGTH;VIN=(YIN-YC)/LENGTH;
WIN=SQRT(1-UIN**2-VIN**2);
                    "gb 01/2000"
                    "MODIFIED 08/07/2000"
;
IF(IWATCH>0)[OUTPUT
1,EIN,IQIN,IRIN,XIN,YIN,ZIN,UIN,VIN,WIN,LATCHI,WTIN;
(' INITIAL SHOWER VALUES',T36,':',I2,F15.6,2I4,3F8.3,3F7.3,I10,1PE10.3);]
;
DO II=1,$MXSTACK[LASTIR(II)=0;LATCH(NP)=0]"ZEROING NEW VARIABLE
THAT TRACKS"
"THE REGION OF THE PREVIOUS INTERACTION   GB-TAGS 16/06/2000"

CALL SHOWER (IQIN,EIN,XIN,YIN,ZIN,UIN,VIN,WIN,IRIN,WTIN);

IF(IWATCH ~= 0)[CALL WATCH(-1,IWATCH);]
]"END OF LOOP ON CASES"
```

```
]"END OF LOOP ON BATCHES"
;
"OUTPUT61;('0ETOTIN,IQIN,  NCASE, IWATCH,TIMMAX,  INSEED'/'$: '); "
"OUTPUT61 ETOTIN,IQIN,NCASE,IWATCH,TIMMAX,INSEED;              "
"('+',F12.6,I10,I8,I6,F7.2,I14);                    "
OUTPUT61;('0ETOTIN,IQIN,  NCASE, IWATCH,TIMMAX,  INSEED,ZIN'/'$: ');
OUTPUT61 ETOTIN,IQIN,NCASE,IWATCH,TIMMAX,INSEED,ZIN;
('+',F15.6,I10,I8,I6,F7.2,I14,F7.2);
          "GB-TAGS 06/07/2000"

$SET_ELAPSED_CPUTIME(CPUT1);
TIMCPU=$CONVERSION_TO_SECONDS*(CPUT1-CPUT0);
OUTPUT61 TIMCPU,TIMCPU/3600.;('0TOTAL CPUTIME FOR
SIMULATIONS=',
F10.1,' s  =',F10.3,' hr'/);


%E
"STEP 8 ANALYSE RESULTS"
"======================"
/TNPRIME,TNCOMPT,TNBREM,TNANNIH,TNCHPART/=0;
/TEPRIME,TECOMPT,TEBREM,TEANNIH,TECHPART/=0.0;

DO IS=1,$STAT[
TNPRIME=TNPRIME+SNPRIME(IS);
TEPRIME=TEPRIME+SEPRIME(IS);
TNCOMPT=TNCOMPT+SNCOMPT(IS);
TECOMPT=TECOMPT+SECOMPT(IS);
TNBREM=TNBREM+SNBREM(IS);
TEBREM=TEBREM+SEBREM(IS);
```

```
TNANNIH=TNANNIH+SNANNIH(IS);
TEANNIH=TEANNIH+SEANNIH(IS);
TNCHPART=TNCHPART+SNCHPART(IS);
TECHPART=TECHPART+SECHPART(IS);]

"resulting total number of particles with energies:"
"we need this for the output "
RNPRIME=TNPRIME;
REPRIME=TEPRIME;
RNCOMPT=TNCOMPT;
RECOMPT=TECOMPT;
RNBREM=TNBREM;
REBREM=TEBREM;
RNANNIH=TNANNIH;
REANNIH=TEANNIH;
RNCHPART=TNCHPART;
RECHPART=TECHPART;

ISTAT=$STAT; STAT=ISTAT; SDENOM=(STAT-1);

;
"MEAN"
TNPRIME=TNPRIME/STAT;
TEPRIME=TEPRIME/STAT;
TNCOMPT=TNCOMPT/STAT;
TECOMPT=TECOMPT/STAT;
TNBREM=TNBREM/STAT;
TEBREM=TEBREM/STAT;
TNANNIH=TNANNIH/STAT;
TEANNIH=TEANNIH/STAT;
```

```
TNCHPART=TNCHPART/STAT;
TECHPART=TECHPART/STAT;
            "NEED AVERAGE PER BATCH - HENCE /STAT"
 "NOW UNCERTAINTIES CALCULATED FOR EACH QUANTITY GB-TAGS
31/07/2000"

/UNPRIME,UNCOMPT,UNBREM,UNANNIH,UNCHPART/=0;
/UEPRIME,UECOMPT,UEBREM,UEANNIH,UECHPART/=0.0;
        DO IS=1,ISTAT[
        UNPRIME=UNPRIME+(SNPRIME(IS)-TNPRIME)**2;
        UEPRIME=UEPRIME+(SEPRIME(IS)-TEPRIME)**2;
        UNCOMPT=UNCOMPT+(SNCOMPT(IS)-TNCOMPT)**2;
        UECOMPT=UECOMPT+(SECOMPT(IS)-TECOMPT)**2;
        UNBREM=UNBREM+(SNBREM(IS)-TNBREM)**2;
        UEBREM=UEBREM+(SEBREM(IS)-TEBREM)**2;
        UNANNIH=UNANNIH+(SNANNIH(IS)-TNANNIH)**2;
        UEANNIH=UEANNIH+(SEANNIH(IS)-TEANNIH)**2;
        UNCHPART=UNCHPART+(SNCHPART(IS)-TNCHPART)**2;
        UECHPART=UECHPART+(SECHPART(IS)-TECHPART)**2;
                ]
UNPRIME=SQRT(UNPRIME/STAT/SDENOM);
UEPRIME=SQRT(UEPRIME/STAT/SDENOM);
UNCOMPT=SQRT(UNCOMPT/STAT/SDENOM);
UECOMPT=SQRT(UECOMPT/STAT/SDENOM);
UNBREM=SQRT(UNBREM/STAT/SDENOM);
UEBREM=SQRT(UEBREM/STAT/SDENOM);
UNANNIH=SQRT(UNANNIH/STAT/SDENOM);
UEANNIH=SQRT(UEANNIH/STAT/SDENOM);
UNCHPART=SQRT(UNCHPART/STAT/SDENOM);
UECHPART=SQRT(UECHPART/STAT/SDENOM);
```

```
;
%E
"     OUTPUT RESULTS"
"     ==============="

"NEW CODE                          GB-TAGS 26/04/2000      "
"TOTAL NUMBER OF PRIMARIES"
OUTPUT61 NCASE,ETOTIN; (' TOTAL PRIMARY PHOTONS INCIDENT',I10,
'INCIDENT ENERGY',F15.6);
OUTPUT61 RNPRIME,UNPRIME,UNPRIME/RNPRIME*100;
(' NR PRIMARY PHOTONS SCORED:',F15.2,'  ABS.ERR:',F10.4,'
PREC.ERR:',F8.4,'%');
OUTPUT61 REPRIME,UEPRIME,UEPRIME/REPRIME*100;
(' EN PRIMARY PHOTONS SCORED:',F15.6,'  ABS.ERR:',F10.4,'
PREC.ERR:',F8.4,'%');
OUTPUT61 RNBREM,UNBREM,UNBREM/RNBREM*100;
(' NR BREM PHOTONS SCORED:  ',F15.2,'  ABS.ERR:',F10.4,'
PREC.ERR:',F8.4,'%');
OUTPUT61 REBREM,UEBREM,UEBREM/REBREM*100;
(' EN BREM PHOTONS SCORED:  ',F15.6,'  ABS.ERR:',F10.4,'
PREC.ERR:',F8.4,'%');
OUTPUT61 RNCOMPT,UNCOMPT,UNCOMPT/RNCOMPT*100;
(' NR COMPT PHOTONS SCORED:  ',F15.2,'  ABS.ERR:',F10.4,'
PREC.ERR:',F8.4,'%');
OUTPUT61 RECOMPT,UECOMPT,UECOMPT/RECOMPT*100;
(' EN COMPT PHOTONS SCORED:  ',F15.6,'  ABS.ERR:',F10.4,'
PREC.ERR:',F8.4,'%');
OUTPUT61 RNANNIH,UNANNIH,UNANNIH/RNANNIH*100;
```

```
(' NR ANNIH PHOTONS SCORED:  ',F15.2,'  ABS.ERR:',F10.4,'
PREC.ERR:',F8.4,'%');
OUTPUT61 REANNIH,UEANNIH,UEANNIH/REANNIH*100;
(' EN ANNIH PHOTONS SCORED:  ',F15.6,'  ABS.ERR:',F10.4,'
PREC.ERR:',F8.4,'%');
OUTPUT61 RNCHPART,UNCHPART,UNCHPART/RNCHPART*100;
(' NR CHARGED PART SCORED:   ',F15.2,'  ABS.ERR:',F10.4,'
PREC.ERR:',F8.4,'%');
OUTPUT61 RECHPART,UECHPART,UECHPART/RECHPART*100;
(' EN CHARGED PART SCORED:   ',F15.6,'  ABS.ERR:',F10.4,'
PREC.ERR:',F8.4,'%');
OUTPUT61 RNPRIME/FLOAT(NCASE),REPRIME/ETOTIN;
(' FRACTION PRIMARIES SCORED:',F15.6,'  FRACTION PRIM EN SCORED:
',F10.6);
TNSCAT=RNBREM+RNCOMPT+RNANNIH+RNCHPART;
TESCAT=REBREM+RECOMPT+REANNIH+RECHPART;
OUTPUT61 TNSCAT,TESCAT;
(' TOTAL NR OF SCATTER:',F12.2,'  TOTAL EN. OF SCATTER:  ',F12.6);
UNSCAT=UNBREM+UNCOMPT+UNANNIH+UNCHPART;
UESCAT=UEBREM+UECOMPT+UEANNIH+UECHPART;
OUTPUT61 UNSCAT,UESCAT;
(' ABS ERR. NR OF SCAT:',F12.4,'  ABS ERR EN. OF SCAT:  ',F12.6);
OUTPUT61 UNSCAT/TNSCAT*100,UESCAT/TESCAT*100;
(' % ERR. NR OF SCAT:',F12.4,'%',' % ERR EN. OF SCAT:  ',F12.6,'%');

" GB-TAGS 26/04/2000  "
;
CALL PRNTER(12,6,6,1);"RESET PRINTER"  STOP;END;
%E
"*****************************************************************************"
```

```
"                                                    "
"          AUSGAB                                      "
"          ======                                    "
"                                                    "
SUBROUTINE AUSGAB(IARG);
"                                                    "
"*********************************************************************"
;COMIN/EPCONT,GEOM,SCORE,STACK/;

IF(IWATCH ~=0) CALL WATCH(IARG,IWATCH); "IWATCH PASSED IN COMIN
SCORE"

;MXNP=MAX(MXNP,NP); "KEEP TRACK OF HOW DEEP STACK GETS"
IF(NP>=$MXSTACK)[OUTPUT61;(//' IN AUSGAB, NP=',I3,' >= MAXIMUM
STACK',
' ALLOWED WHICH IS',I3/1X,79('*')//);]
IF(MXNP>$MXSTACK)[STOP;"MUST INCREASE $MXSTACK"]
;
;
"WE USE IR(NP) FROM STACK"

"NEW CODE                                    GB-TAGS 26/04/2000"
"  FIRST SET FLAGS WHEN SCATTERING EVENTS OCCUR - IAUSFL WAS
SET "
"  IN STEP 5 OF MAIN TO ENSURE AUSGAB WAS CALLED AT THESE
POINTS "
;
IF(IARG.EQ.7)    [
"Returned to ELECTR after a call to BREMS was made              "
"Check which particle is on top of the stack and just below      "
```

```
   IF(IQ(NP)=0)[
   LATCH(NP)=1; LASTIR(NP)=IR(NP);
          ]
   ELSE       [
   LATCH(NP-1)=1;LASTIR(NP-1)=IR(NP-1);
          ]
           ]
IF(IARG.EQ.18)     [
"Returned to PHOTON after a call to COMPT was made              "
"Check which particle is on top of the stack and just below      "
   IF(IQ(NP).EQ.0) [
   LATCH(NP)=2;LASTIR(NP)=IR(NP);
            ]
   ELSE        [
   LATCH(NP-1)=2;LASTIR(NP-1)=IR(NP-1);
            ]
             ]

IF(IARG.EQ.13.OR.IARG.EQ.14)     [
"Returned to ELECTR after a call to ANNIH was made              "
   LATCH(NP)=3;LASTIR(NP)=IR(NP);
   LATCH(NP-1)=3;LASTIR(NP-1)=IR(NP-1);
                        ]
;
IF(IARG.EQ.3.AND.(IR(NP).EQ.IRS1.OR.IR(NP).EQ.IRS2.OR.IR(NP).EQ.IRS3.
OR.
IR(NP).EQ.IRS4))[
"Particle entering the scoring region                           "
"Only output information for particles that are discarded       "
```

```
WRITE(20,*)E(NP),X(NP),Y(NP),Z(NP),U(NP),V(NP),W(NP),IQ(NP),LASTIR(NP)
,LATCH(NP);
;
IF(IQ(NP).NE.0)[ "AN ELECTRON OR POSITRON"
   SNCHPART(IS)=SNCHPART(IS)+1;
   SECHPART(IS)=SECHPART(IS)+E(NP);
        ]
ELSE       [
    IF(LATCH(NP).EQ.0) [
      "NO SCATTERING - A PRIMARY  "
      SNPRIME(IS)=SNPRIME(IS)+1;
      SEPRIME(IS)=SEPRIME(IS)+E(NP);
              ]
    IF(LATCH(NP).EQ.1)     [
      "IT IS A BREMSSTRAHLUNG PHOTON"
      SNBREM(IS)=SNBREM(IS)+1;
      SEBREM(IS)=SEBREM(IS)+E(NP);
                  ]
;
    IF(LATCH(NP).EQ.2)         [
      "IT IS A COMPTON SCATTERD PHOTON"
      SNCOMPT(IS)=SNCOMPT(IS)+1;
      SECOMPT(IS)=SECOMPT(IS)+E(NP);
                  ]
    IF(LATCH(NP).EQ.3)         [
      "IT IS A POSITRON ANNIHILATION"
      SNANNIH(IS)=SNANNIH(IS)+1;
      SEANNIH(IS)=SEANNIH(IS)+E(NP);
                  ]
        ]
```

]"END SCORING REGION BLOCK"

;

RETURN;END;

%E

```
"*************************************************************************"
"                                                                         "
"              HOWFAR                                                     "
"              ======                                                     "
"                                                                         "
;SUBROUTINE HOWFAR;

"  HOWFAR routine to use with a generalized cartesian coordinate system  "
"                                                                         "
"  Routine is optimized for speed - please suggest improvements          "
"                                                                         "
"  Geometrical information is passed in COMIN/GEOM/                       "
"
XBOUND($IMAX),YBOUND($JMAX),ZBOUND($KMAX),IMAX,JMAX,KMAX,IJM
AX,IRMAX "
"    XBOUND etc are the X, Y and Z boundaries defining the voxels       "
"    $IMAX etc are the maximum number of elements in each direction     "
"         as defined in the users main program                          "
"    IMAX etc are the actual number of elements in each direction for   "
"         this particular calculation                                   "
"    IJMAX = IMAX*JMAX  a useful number                                 "
"    IRMAX = 1 + IJMAX*IKMAX  the total number of regions in the        "
"         current problem                                               "
```

```
"                                                                    "
"   Each voxel is defined by a triple of integers (I,J,K) (but called  "
"        IRX,IRY and IRZ in this routine) such that:                 "
"                                                                    "
"        XBOUND(I) <= X < XBOUND(I+1)    1 < I < IMAX               "
"        YBOUND(J) <= Y < YBOUND(J+1)    1 < J < JMAX               "
"        ZBOUND(K) <= Z < ZBOUND(K+1)    1 < K < KMAX               "
"                                                                    "
" The X axis is up the page, the Y axis to the right and Z into the page "
"                                                                    "
" The region number is defined as:                                   "
"    IR = 1 + I + (J-1)*IMAX + (K-1)*IJMAX                          "
"                                                                    "
" The routine sets DNEAR  Note that in problems where the typical    "
" step size is of the order of the region dimensions, then computing  "
" DNEAR can decrease efficiency. In this case the two lines containing  "
" DNEAR should be commented out                                      "
"                                                                    "
" The routine assumes $DECODEIR(IRL,I,J,K) is expanded to calculate  "
"        I,J,K given IRL, the current region                         "
"                                                                    "
" Equivalence statements are used to allow variable names to be used  "
"        in the main macro for each direction                        "
"                                                                    "
" Version 1    April 1986  D.W.O.Rogers, NRCC                        "
"                                                                    "
"********************************************************************"

;COMIN/EPCONT,GEOM,STACK/;
REAL XCOS($MXSTACK),YCOS($MXSTACK),ZCOS($MXSTACK);
```

```
EQUIVALENCE (XCOS,U), (YCOS,V), (ZCOS,W);
EQUIVALENCE (MAXX,IMAX), (MAXY,JMAX), (MAXZ,KMAX);
EQUIVALENCE (IRDELX,IONE),(IRDELY,IMAX),(IRDELZ,IJMAX);
"  IRDELn is the change in region number as cross boundary in the"
"   direction specified by n"
DATA IONE/1/;  "placed this after equivalence stmt Dec 31, 1996 DR"

%E
" Define a macro which does the geometry check for one direction"

"  note that this macro assumes IRL has been decoded to IRX,IRY,IRZ instead"
"  of the more usual I,J,K, it assumes IRL = IR(NP) and DNEAR is set      "
"  very large before the first call                                       "

REPLACE {$CHECK-IN-#-DIRECTION;} WITH
"      ======================"

{"note current region has {P1}BOUND(IR{P1} <= {P1} < {P1}BOUND(IR{P1}+1)"

DNEARL=MIN(DNEARL,({P1}BOUND(IR{P1}+1)-{P1}(NP)),({P1}(NP)-
{P1}BOUND(IR{P1})));

IF( {P1}COS(NP) > 0.0)["going towards outer plane"
   DIST = ({P1}BOUND(IR{P1}+1)-{P1}(NP))/{P1}COS(NP);"Distance to
boundary"

   IF(DIST < USTEP) [USTEP=DIST;
      IF(IR{P1} ~= MAX{P1})[IRNEW=IRL+IRDEL{P1};]
         ELSE ["leaving entire geometry" IRNEW=1;]
"  note this only assigns IRNEW correctly                                 "
```

```
"  if no other boundaries are crossed first - but                "
"  if they are, IRNEW will be set correctly there                "
   ]"end of block to reduce USTEP"
]"end of COS > 0 branch"

ELSEIF({P1}COS(NP) < 0.0) ["going towards inner plane"
   DIST = -( {P1}(NP) - {P1}BOUND(IR{P1}))/{P1}COS(NP);
   IF(DIST < USTEP) [USTEP = DIST;
      IF(IR{P1} ~= 1)[IRNEW=IRL-IRDEL{P1};]
         ELSE ["leaving geometry" IRNEW = 1;]]
]"end of COS < 0 branch"

"note, no COS = 0 branch needed since cannot cross boundary"

}"end of macro replacement"


;IRL = IR(NP);  IF(IRL.EQ.1.OR.IRL.EQ.IRS1.OR.IRL.EQ.IRS2.OR.
IRL.EQ.IRS3.OR.IRL.EQ.IRS4)[ IDISC = 1;RETURN;]
"have left geometry"
$DECODEIR(IRL,IRX,IRY,IRZ);
DNEARL = 1.E10;
"OUTPUT61;('0IRL, IRNEW, IDISC, USTEP, X, Y, Z, U, V, W'/'$: ');"
"OUTPUT61 IRL, IRNEW, IDISC, USTEP, X(NP), Y(NP), Z(NP),U(NP),
V(NP),W(NP);"
"('+',I8,I8,I3,F12.3,F8.3,F8.3,F8.3,F8.3,F8.3,F8.3);"
$CHECK-IN-Z-DIRECTION;
"OUTPUT61;(' CHECK IN Z DIRECTION'/'$: '); "
"OUTPUT61 IRL, IRNEW, IDISC, USTEP, X(NP), Y(NP), Z(NP), U(NP), V(NP),
W(NP);"
```

```
"('+',I8,I8,I3,F12.3,F8.3,F8.3,F8.3,F8.3,F8.3,F8.3);"
$CHECK-IN-X-DIRECTION;
"OUTPUT61 IRL, IRNEW, IDISC, USTEP, X(NP), Y(NP), Z(NP), U(NP), V(NP),
W(NP);"
"('+',I8,I8,I3,F12.3,F8.3,F8.3,F8.3,F8.3,F8.3,F8.3);"
$CHECK-IN-Y-DIRECTION;
"OUTPUT61 IRL, IRNEW, IDISC, USTEP, X(NP), Y(NP), Z(NP), U(NP), V(NP),
W(NP);"
"('+',I8,I8,I3,F12.3,F8.3,F8.3,F8.3,F8.3,F8.3,F8.3);"

DNEAR(NP) = DNEARL;
RETURN;END;
```

APPENDIX B: Commented Input File

The following example is for the 6.37cm thick aluminum attenuator for the $1x1cm^2$ field.

6 MV photon beam -6.37cm thick attenuator-1x1sqcm field

4 "number of media"
AIR
ALUMINUM
CERROBEND
CONCRETE
0.521,0.010,0.01,0.01,0.01,0.01 "cut-off energies:AE,AP"
17,15,33 "number of regions in x,y,z directions"
0.0 "regions on the x-direction"
2.0
124.5
127.0
129.0
130.5
130.75
131.0
131.3265 } "detector region"
132.6735
133.0
133.25
133.5
135.0
137.0
139.5

277.0
279.0
0.0 "regions on the y-direction"
2.0
404.5
407.0
409.0
410.5
410.75
411.0
413.0
413.25 "detector region"
413.5
413.9
417.0
419.5
812.0
814.0
75.0 "regions on the z-direction"
76.0
78.2
80.0
81.37
83.0
84.56
86.0
87.75
89.0
90.94
92.0

94.13
95.0
96.24
98.0
99.42
101.0
103.88
104.0
105.79
107.06
110.89
112.17
117.27
118.55
121.73
230.0
235.0
240.0
330.0 } "detector region"
331.347
475.0
477.0 "Beam's eye view: density of each media is defined"
1,17,1,15,1,33,1,0.001
1,17,1,1,1,33,4,2.26 "left wall: concrete"
1,17,15,15,1,33,4,2.26 "right wall: concrete"
1,1,1,15,1,33,4,2.26 "floor: concrete"
17,17,1,15,1,33,4,2.26 "ceiling: concrete"
1,17,1,15,33,33,4,2.26 "back wall: concrete"
3,15,3,13,1,4,2,2.702 "6.37cm attenuator: aluminum"

4,5,4,12,28,29,3,9.76
6,6,4,7,28,29,3,9.76
6,6,9,12,28,29,3,9.76
7,7,4,6,28,29,3,9.76
7,7,10,12,28,29,3,9.76
8,10,4,5,28,29,3,9.76
8,10,11,12,28,29,3,9.76
11,11,4,6,28,29,3,9.76
11,11,10,12,28,29,3,9.76
12,12,4,7,28,29,3,9.76
12,12,9,12,28,29,3,9.76
13,14,4,12,28,29,3,9.76

"extra collimator: cerrobend"

9,9,8,11,31,31,1,0.001 "scoring regions: air"

0,0,0,0,0,0,0,0.0

9,9,8,8,31,31
9,9,9,9,31,31
9,9,10,10,31,31
9,9,11,11,31,31

"scoring regions"

131.625,132.375 "x-coordinates of the field"

411.625,412.375 "y-coordinates of the field"

0,1000000,0,0.0,0,75.0